JAK inhibition decreases the autoimmune burden in Down syndrome

Author list: Angela L. Rachubinski[1,2*], Elizabeth Wallace[3], Emily Gurnee[3], Belinda A. Enriquez Estrada[1], Kayleigh R. Worek[1], Keith P. Smith[1], Paula Araya[1], Katherine A. Waugh[1,4], Ross E. Granrath[1], Eleanor Britton[1], Hannah R. Lyford[1], Micah G. Donovan[1,5], Neetha Paul Eduthan[1], Amanda A. Hill[1], Barry Martin[6], Kelly D. Sullivan[1,7], Lina Patel[1,8], Deborah J. Fidler[9], Matthew D. Galbraith[1,5], Cory A. Dunnick[3], David A. Norris[3], Joaquin M. Espinosa[1,5*].

Affiliations:

[1]Linda Crnic Institute for Down Syndrome, University of Colorado Anschutz Medical Campus, Aurora, CO, USA.

[2]Department of Pediatrics, Section of Developmental Pediatrics, University of Colorado Anschutz Medical Campus, Aurora, CO, USA.

[3]Department of Dermatology, University of Colorado Anschutz Medical Campus, Aurora, CO, USA.

[4]Current address: Department of Cell Biology and Physiology, University of Kansas Medical Center, Kansas City, KS, USA.

[5]Department of Pharmacology, University of Colorado Anschutz Medical Campus, Aurora, CO, USA

[6]Department of Internal Medicine, University of Colorado Anschutz Medical Campus, Aurora, CO, USA.

[7]Department of Pediatrics, Section of Developmental Biology, University of Colorado Anschutz Medical Campus, Aurora, CO, USA.

[8]Department of Psychiatry, Child and Adolescent Division, University of Colorado Anschutz Medical Campus, Aurora, CO, USA.

[9]Department of Human Development and Family Studies, Colorado State University, Fort Collins, CO, USA.

*Corresponding authors:

joaquin.espinosa@cuanschutz.edu / angela.rachubinski@cuanschutz.edu

Abstract.

Individuals with Down syndrome (DS), the genetic condition caused by trisomy 21 (T21), display clear signs of immune dysregulation, including high rates of autoimmune disorders and severe complications from infections. Although it is well established that T21 causes increased interferon responses and JAK/STAT signaling, elevated autoantibodies, global immune remodeling, and hypercytokinemia, the interplay between these processes, the clinical manifestations of DS, and potential therapeutic interventions remain ill defined. Here, we report a comprehensive analysis of immune dysregulation at the clinical, cellular, and molecular level in hundreds of individuals with DS. We demonstrate multi-organ autoimmunity of pediatric onset concurrent with unexpected autoantibody-phenotype associations. Importantly, constitutive immune remodeling and hypercytokinemia occur from an early age prior to autoimmune diagnoses or autoantibody production. We then report the interim analysis of a Phase II clinical trial investigating the safety and efficacy of the JAK inhibitor tofacitinib through multiple clinical and molecular endpoints. Analysis of the first 10 participants to complete the 16-week study shows a good safety profile and no serious adverse events. Treatment reduced skin pathology in alopecia areata, psoriasis, and atopic dermatitis, while decreasing interferon scores, cytokine scores, and levels of pathogenic autoantibodies without overt immune suppression. Additional research is needed to define the effects of JAK inhibition on the broader developmental and clinical hallmarks of DS. ClinicalTrials.gov identifier: NCT04246372.

46 **Introduction.**

47 Trisomy of human chromosome 21 (T21) occurs at a rate of ~1 in 700 live births, causing Down
48 syndrome (DS)[1,2]. Individuals with DS display a distinct clinical profile including developmental delays,
49 stunted growth, cognitive impairments, and increased risk of leukemia, autism spectrum disorders, seizure
50 disorders, and Alzheimer's disease[2,3]. People with DS also display widespread immune dysregulation,
51 which manifests through severe complications from respiratory viral infections and high prevalence of
52 myriad immune conditions, including autoimmune thyroid disease (AITD)[4-6], celiac disease[7,8], and skin
53 conditions such as atopic dermatitis, alopecia areata, hidradenitis suppurativa (HS), vitiligo, and psoriasis[9-
54 11]. Furthermore, people with DS display signs of neuroinflammation from an early age[12-14]. Although it is
55 now well accepted that immune dysregulation is a hallmark of DS, the underlying mechanisms and
56 therapeutic implications are not yet fully defined.

57 We previously reported that T21 causes consistent activation of the interferon (IFN) transcriptional
58 response in multiple immune and non-immune cell types with concurrent hypersensitivity to IFN
59 stimulation and hyperactivation of downstream JAK/STAT signaling[15-17]. Plasma proteomics studies
60 identified dozens of inflammatory cytokines with mechanistic links to IFN signaling that are elevated in
61 people with DS[18]. A large metabolomics study revealed that T21 drives the production of neurotoxic
62 tryptophan catabolites via the IFN-inducible kynurenine pathway[19]. Deep immune profiling revealed
63 global immune remodeling with hypersensitivity to IFN across all major branches of the immune system[15],
64 and dysregulation of T cell lineages toward a hyperactive, autoimmunity-prone state[16]. These results could
65 be partly explained by the fact that four of the six IFN receptors (IFNRs) are encoded on chr21, including
66 Type I, II and III IFNR subunits[20]. In a mouse model of DS, normalization of *IFNR* gene copy number
67 rescues multiple phenotypes of DS, including lethal immune hypersensitivity, congenital heart defects
68 (CHDs), cognitive impairments, and craniofacial anomalies[21]. JAK inhibition rescues lethal immune
69 hypersensitivity in these mouse models[22] and attenuates the global dysregulation of gene expression
70 caused by the trisomy across multiple murine tissues[23]. Furthermore, prenatal JAK inhibition in pregnant

71 mice prevents the appearance of CHDs[24]. Altogether, these results support the notion that T21 elicits an
72 interferonopathy in DS, and that pharmacological inhibition of IFN signaling could have multiple
73 therapeutic benefits in this population.

74 Although it is now well established that T21 disrupts immune homeostasis toward an autoimmunity-
75 prone state, the interplay between overexpression of chromosome 21 genes, hyperactive interferon
76 signaling, dysregulation of immune cell lineages, autoantibody production, hypercytokinemia, and the
77 various developmental and clinical features of DS remain to be elucidated. Previous studies established
78 similarities between the immune profiles of typical aging, autoimmunity in the general population, and
79 DS, proposing a role for accelerated immune aging in the pathophysiology of DS[25-27]. Other studies
80 indicate a role for elevated cytokine production, hyperactivated T cells, and ongoing B cell activation as
81 drivers of autoimmunity in DS[15,16,28]. However, given the relatively small sample sizes and observational
82 nature of these studies, it has not been possible to define the contribution of specific dysregulated events
83 to breach of tolerance leading to clinically evident autoimmunity in DS. Therefore, additional research is
84 needed to define driver versus bystander events that could illuminate therapeutic strategies to decrease the
85 burden of autoimmunity in DS.

86 Within this context, we report here a comprehensive analysis of the immune disorder of DS, including
87 detailed annotation of autoimmune and inflammatory conditions and quantification of autoantibodies in
88 hundreds of research participants, which reveals widespread autoimmune attack on all major organ
89 systems in DS from an early age, including unexpected autoantibody-phenotype associations. Then, using
90 deep immune mapping and quantitative proteomics, we demonstrate that T21 causes widespread immune
91 remodeling toward an autoimmunity-prone state accompanied by hypercytokinemia prior to clinically
92 evident autoimmunity or autoantibody production. Lastly, we report the interim analysis of a clinical trial
93 investigating the safety and efficacy of the JAK1/3 inhibitor tofacitinib (Xeljanz, Pfizer) in DS. These
94 results demonstrate that JAK inhibition improves multiple immunodermatological conditions in DS,
95 normalizes interferon scores, decreases levels of major pathogenic cytokines (e.g., TNF-α, IL-6), and

96 reduces levels of pathogenic autoantibodies [e.g., anti-thyroid peroxidase (anti-TPO)]. Altogether, these
97 results point to hyperactive JAK/STAT signaling as driver of autoimmunity in DS and justify the ongoing
98 trials of JAK inhibitors in DS for multiple clinical endpoints.
99

100 **Results.**

101 **Widespread multi-organ autoimmunity and autoantibody production in Down syndrome.**

102 Previous studies have documented increased rates of diverse autoimmune conditions in DS relative to
103 the general population including autoimmune thyroid disease (AITD)[29], celiac disease[30], autoimmune skin
104 conditions[9-11], and type I diabetes[31,32]. However, many of these studies were limited by relatively small
105 sample sizes, independent analysis of individual autoimmune conditions, or a focus on specific age ranges.
106 In order to complete a more comprehensive analysis of autoimmune conditions in DS across the lifespan,
107 we analyzed the harmonized clinical profiles of 441 research participants with DS, aged 6 months to 57
108 years, enrolled in the Human Trisome Project cohort study (HTP, NCT02864108), which annotates
109 clinical data through a combination of participant/caregiver surveys and expert abstraction of electronic
110 health records (EHRs) (see **Materials and Methods**, **Supplementary file 1**). In this analysis, the most
111 common autoimmune condition is AITD, affecting 53.1% of the total cohort (**Figure 1a**, **Figure 1 – figure**
112 **supplement 1a**). Grouped together, autoimmune and inflammatory skin conditions represent the second
113 most common category, affecting 43% of the cohort, including: atopic dermatitis / eczema (27.9%),
114 hidradenitis suppurativa / folliculitis / boils (20.6%), alopecia areata (7.7%), psoriasis (6.1%), and vitiligo
115 (1.9%) (**Figure 1a**, **Figure 1 - supplement 1b**). The rate of celiac disease (9.6%) is also highly elevated
116 over that of the general population[33]. We observed 10 cases (2.2%) of juvenile Type I diabetes, which has
117 been reported to be more common in DS[31,32]. Other autoimmune conditions common in the general
118 population, such as systemic lupus erythematosus or multiple sclerosis, were not observed in the HTP
119 cohort.

120 In the general population, the risk of autoimmune conditions increases with age and is higher in
121 females, with autoimmune conditions tending to cluster, whereby occurrence of one autoimmune
122 condition predisposes to a second condition[34,35]. Within the HTP cohort, analysis of age trajectories of
123 immune-related conditions in DS revealed early onset, with >80% of AITD, autoimmune/inflammatory
124 skin conditions, and celiac disease being diagnosed in the first two decades of life (**Figure 1 - supplement**

125 **1c-e**). The cumulative burden of autoimmunity and autoinflammation is similar in males versus females
126 with DS, albeit with slightly increased rates of AITD and hidradenitis suppurativa in females (**Figure 1 -**
127 **supplement 1f**). In terms of co-occurrence, when evaluating the adult population (18+ years old) for
128 AITD, autoimmune/inflammatory skin conditions and celiac disease, we found that 75% of participants
129 had a history of at least one condition, 38.4% had at least two, and 13.6% had three or more conditions
130 (**Figure 1b**).

131 Interestingly, analysis of medical records found an unexpectedly low number of individuals with
132 records of autoantibodies against the thyroid gland [4.3%, e.g., anti-thyroid peroxidase (TPO), anti-
133 thyroglobulin (TG)] within the HTP cohort (**Figure 1 - supplement 1a**). This could be explained by the
134 fact that thyroid disease is commonly diagnosed through measurements of thyroid-relevant hormones
135 (TSH, T3, T4) without concurrent testing of autoantibodies. To investigate further, we measured anti-TPO
136 levels as well as levels of anti-nuclear antibodies (ANA), a more general biomarker of autoimmunity
137 (**Supplementary file 2**). Remarkably, 82.4% of adults with DS show positivity for at least one of these
138 autoantibodies, with 41.2% being positive for both (**Figure 1c**). Indeed, 62% of individuals with history
139 of hypothyroidism were TPO+, whereby anti-TPO is just one of the possible autoantibodies associated
140 with AITD. Prompted by these results, we next completed a more comprehensive analysis of
141 autoantibodies in DS using protein array technology, with a focus on ~380 common autoepitopes from
142 270 proteins (see **Materials and Methods, Supplementary file 2**). These efforts identified 25
143 autoantibodies significantly over-represented in people with DS relative to age- and sex-matched controls
144 (**Figure 1d**), with 98.3% of individuals with DS being positive for at least one of these autoantibodies,
145 and 63.3% being positive for six or more (**Figure 1d-e**). In addition to autoantibodies against TPO, which
146 is expressed exclusively in the thyroid gland, we identified autoantibodies targeting proteins that are either
147 broadly expressed across multiple tissues (e.g., TOP1, UBA1, LAMP2) or preferentially expressed in
148 specific organs across the human body, including liver (e.g., CYP1A2), pancreas (e.g., SLC30A8), skin
149 (e.g., DSG3), bone marrow (e.g. SRP68), and brain tissue (e.g., AIMP1) (**Figure 1d, f**).

150 Analysis of autoantibody positivity relative to history of co-occurring conditions produced several
151 interesting observations. Expectedly, individuals with hypothyroidism are more likely to be positive for
152 anti-TPO antibodies (**Figure 1g-h**). However, unexpectedly, TPO+ status also associates with higher rates
153 of use of pressure equalizing (PE) tubes employed to alleviate the symptoms of recurrent ear infections
154 and otitis media with effusion (OME), which is common in DS[36] (**Figure 1g-h**). Possible interpretations
155 for this result are provided in the Discussion. Positivity for additional autoantibodies was more common
156 in those with other co-occurring neurological conditions, a broad classification encompassing various
157 seizure disorders, movement disorders, and structural brain abnormalities (**Figure 1g-h, Figure 1 – figure**
158 **supplement 1g**). Salient examples are antibodies against MUSK, a muscle-associated receptor tyrosine
159 kinase involved in clustering of the acetylcholine receptors in the neuromuscular junction[37]; UBA1, a
160 ubiquitin conjugating enzyme involved in antigen presentation[38]; and MYH6, a cardiac myosin heavy
161 chain isoform (**Figure 1g-h**, **Figure 1 – figure supplement 1g**). Individuals with history of tricuspid valve
162 regurgitation display higher rates of four different autoantibodies, most prominently against WARS1, a
163 tryptophan tRNA synthetase mutated in various neurodevelopmental disorders[39], and SRP68, a protein
164 commonly targeted by autoantibodies in necrotizing myopathies[40] (**Figure 1 – figure supplement 1g**).
165 Individuals with a history of frequent pneumonia present a higher frequency of autoantibodies against
166 DSG3 (desmoglein 3), a cell adhesion molecule targeted by autoantibodies in paraneoplastic pemphigus
167 (PNP), an autoimmune disease of the skin and mucous membranes that can involve fatal lung
168 complications[41] (**Figure 1g-h**).
169 Altogether, these results demonstrate widespread multi-organ autoimmunity across the lifespan in
170 people with DS, with production of multiple autoantibodies that could potentially contribute to a number
171 of co-occurring conditions more common in this population.
172

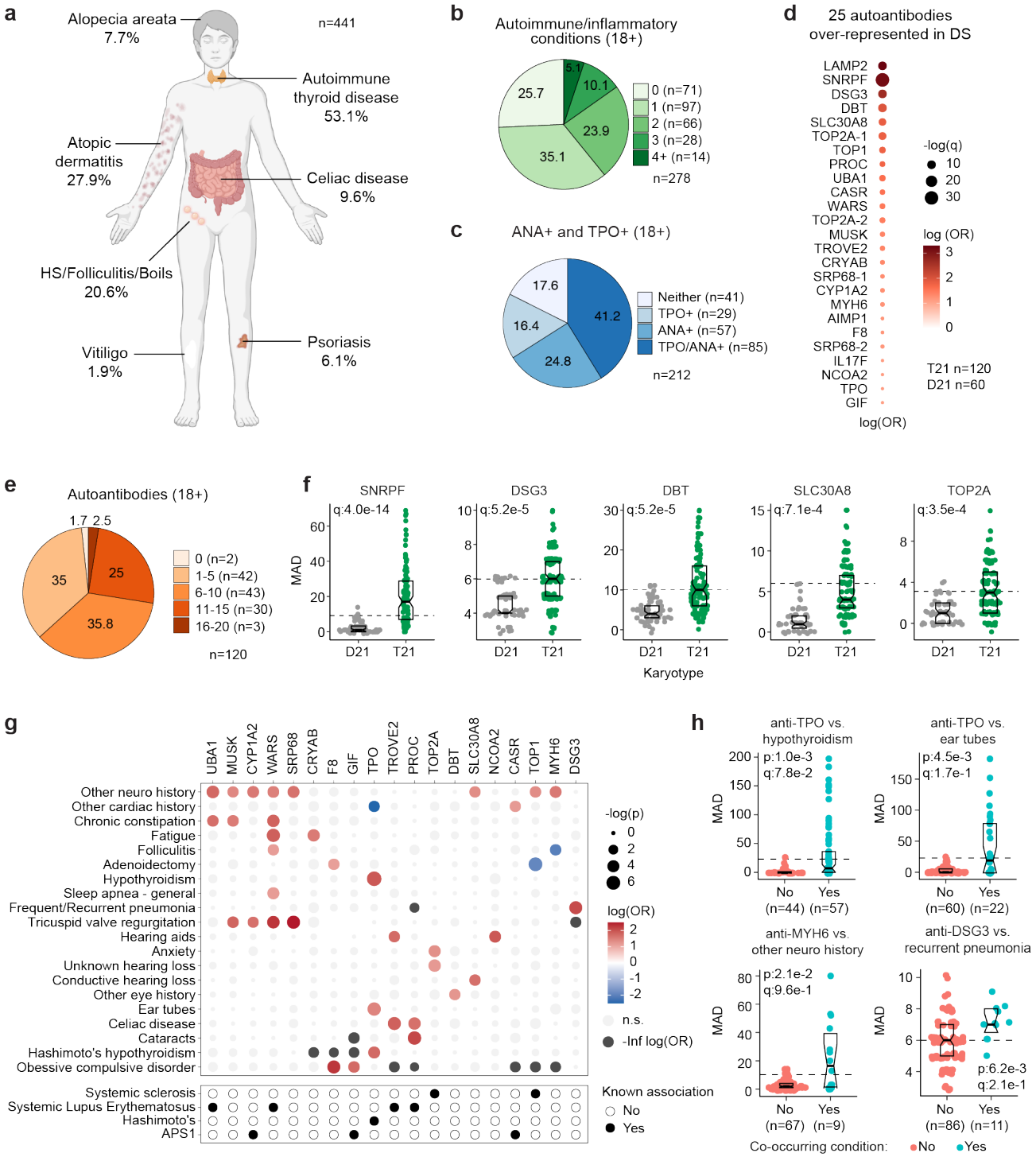

Figure 1. Multi-organ autoimmunity and widespread autoantibody production in Down syndrome. **a,** Overview of autoimmune and inflammatory conditions prevalent in persons with Down syndrome (DS) enrolled in the Human Trisome Project (HTP) cohort study. Percentages indicate the fraction of participants (n=441, all ages) with history of the indicated conditions. **b**, Pie chart showing

178 autoimmune/inflammatory condition burden in adults (n=278, 18+ years old) with DS. **c**, Pie chart
179 showing rates of positivity for anti-TPO and/or anti-nuclear antibodies (ANA) in adults (n=212, 18+ years
180 old) with DS. **d**, Bubble plot displaying odds-ratios and significance for 25 autoantibodies with elevated
181 rates of positivity in individuals with DS (n=120) versus 60 euploid controls (D21). q values calculated
182 by Benjamini-Hochberg adjustment of p-values from Fisher's exact test. **e**, Pie chart showing fractions of
183 adults with DS (n=120, 18+ years old) testing positive for various numbers of the autoantibodies identified
184 in d. **f**, Representative examples of autoantibodies more frequent in individuals with T21 (n=120) versus
185 euploid controls (D21, n=60). MAD: median absolute deviation. Dashed lines indicate the positivity
186 threshold of 90th percentile for D21. Data are presented as modified sina plots with boxes indicating
187 quartiles. **g**, Bubble plots showing the relationship between autoantibody positivity and history of various
188 clinical diagnoses in DS (n=120). Size of bubbles is proportional to -log-transformed p values from
189 Fisher's exact test. **h**, Sina plots displaying the levels of selected autoantibodies in individuals with DS
190 with or without the indicated co-occurring conditions. MAD: median absolute deviation. Dashed lines
191 indicate the positivity threshold of 90th percentile for D21. Sample sizes are indicated under each plot. q
192 values calculated by Benjamini-Hochberg adjustment of p-values from Fisher's exact tests.
193

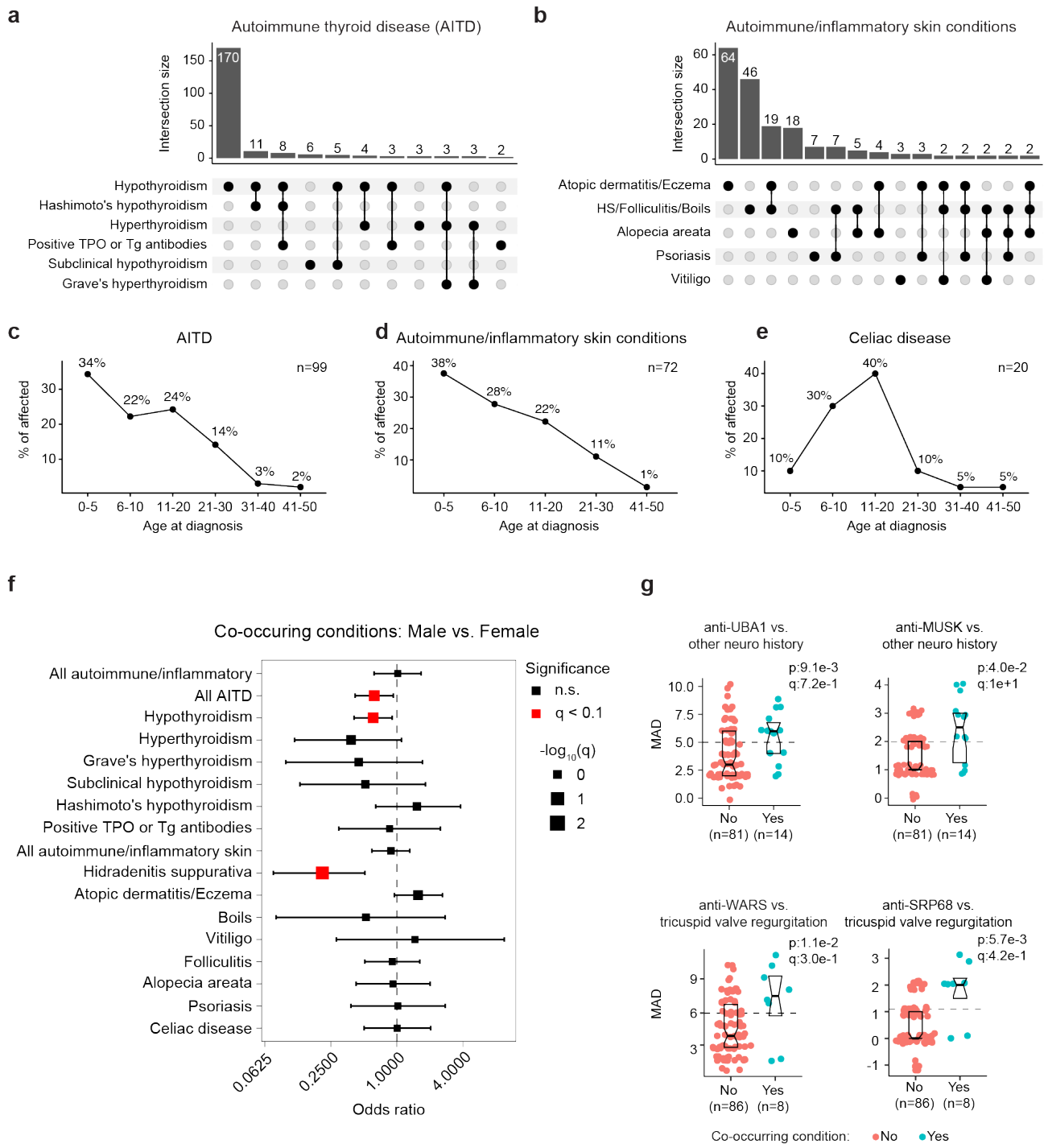

194

195 **Figure 1 – figure supplement 1. Early onset multi-organ autoimmunity and autoantibody**

196 **production in Down syndrome. a-b**, Upset plots showing overlap between various reported diagnoses

197 indicative of autoimmune thyroid disease (a) or autoimmune/inflammatory skin conditions (b) in research

198 participants with Down syndrome (DS, all ages, n=441) enrolled in the Human Trisome Project (HTP). **c-**

e, Plots showing the percentages of cases by age at diagnosis for AITD (c), autoimmune/inflammatory skin conditions (d), and celiac disease (e). Sample sizes indicated in each chart. **f**, Odds ratio plot for Fisher's exact test of proportions (cases vs. controls in males vs. females) for history of co-occurring conditions in individuals with DS (all ages, total n=441). Conditions with $q < 0.1$ (10% FDR) are highlighted in red. The size of square points is inversely proportional to q value; error bars represent 95% confidence intervals. **g**, Sina plots displaying the levels of select autoantibodies in individuals with DS, with or without history of the indicated co-occurring conditions. MAD: median absolute deviation. Horizontal dashed lines indicate 90th percentiles for the D21 group. Sample sizes are indicated under each plot. q values calculated by Benjamini-Hochberg adjustment of p-values from Fisher's exact tests.

209 **Trisomy 21 causes global immune remodeling regardless of evident clinical autoimmunity.**

210 Several immune cell changes have been proposed to underlie the autoimmunity-prone state of
211 DS[15,16,25,42], but specific immune cell-to-phenotype associations have not been established in previous
212 studies using smaller sample sizes. Therefore, we next investigated immune cell changes associated with
213 various clinical and molecular markers of autoimmunity in DS. Toward this end we analyzed mass
214 cytometry data from 292 individuals with DS relative to 96 euploid controls and tested for potential
215 differences in immune cell subpopulations, identified using FlowSOM[43], within the DS cohort based on
216 number of autoimmune/inflammatory disease diagnoses, ANA positivity, TPO positivity, and positivity
217 for additional autoantibodies. In agreement with previous analyses[15,16,25,42], we observed massive immune
218 remodeling in all major myeloid and lymphoid subsets, including increases in basophils, along with
219 depletion of eosinophils and total B cells (**Figure 2a-c, Figure 2 – figure supplement 1a-c**). When
220 comparing various subgroups within the DS cohort based on autoimmunity status, we observed that these
221 global immune changes are largely independent of the presence of clinical diagnoses or autoantibody
222 positivity, with very few additional changes significantly associated with these measures of autoimmunity
223 (**Figure 2 – figure supplement 1d**). For example, the significant depletion of B cells and enrichment of
224 basophils in DS is not significantly different among the various subgroups (**Figure 2c**, **Figure 2 – figure**
225 **supplement 1c**). Among CD45+ CD66^{lo} non-granulocytes, most changes are conserved among
226 subgroups, with the sole of exception of non-classical monocytes, which are further elevated in the ANA+
227 group (**Figure 2 – figure supplement 1d-e**). Among T cells, the overall pattern of depletion of naïve
228 subsets and enrichment of differentiated subsets characteristic of DS[15,16,28,42] is conserved across
229 subgroups, as illustrated by consistent depletion of CD8+ naïve subsets along with increases in the CD8+
230 terminally differentiated effector memory (TEMRA) subset (**Figure 2f, Figure 2 – figure supplement**
231 **1d**). Notably, we observed depletion of γδ T cells (both total and CD8+) in those with multiple
232 autoimmune diagnoses (**Figure 2 – figure supplement 1d, f**), a result that is in line with reports
233 documenting depletion of these subsets from peripheral circulation toward sites of active autoimmunity[44].

234 We also observed slight elevation of CD4+ T central memory cells (TCM) (**Figure 2 – figure supplement**
235 **1d, f**). Among B cells, the overall shift toward more differentiated states such as plasmablasts, age-
236 associated B cells (ABCs), and IgM+ memory cells is also conserved among subgroups, with the sole
237 exception of ABCs, which tend to be further elevated in the TPO+ group (**Figure 2g-i**, **Figure 2 – figure**
238 **supplement 1d, g**).

239 Altogether, these results indicate that T21 causes global remodeling of the immune system toward an
240 autoimmunity-prone and pro-inflammatory state, prior to clinically evident autoimmunity, and dwarfing
241 any additional effects associated with confirmed diagnoses of autoimmune/inflammatory conditions or
242 common biomarkers of autoimmunity.

243

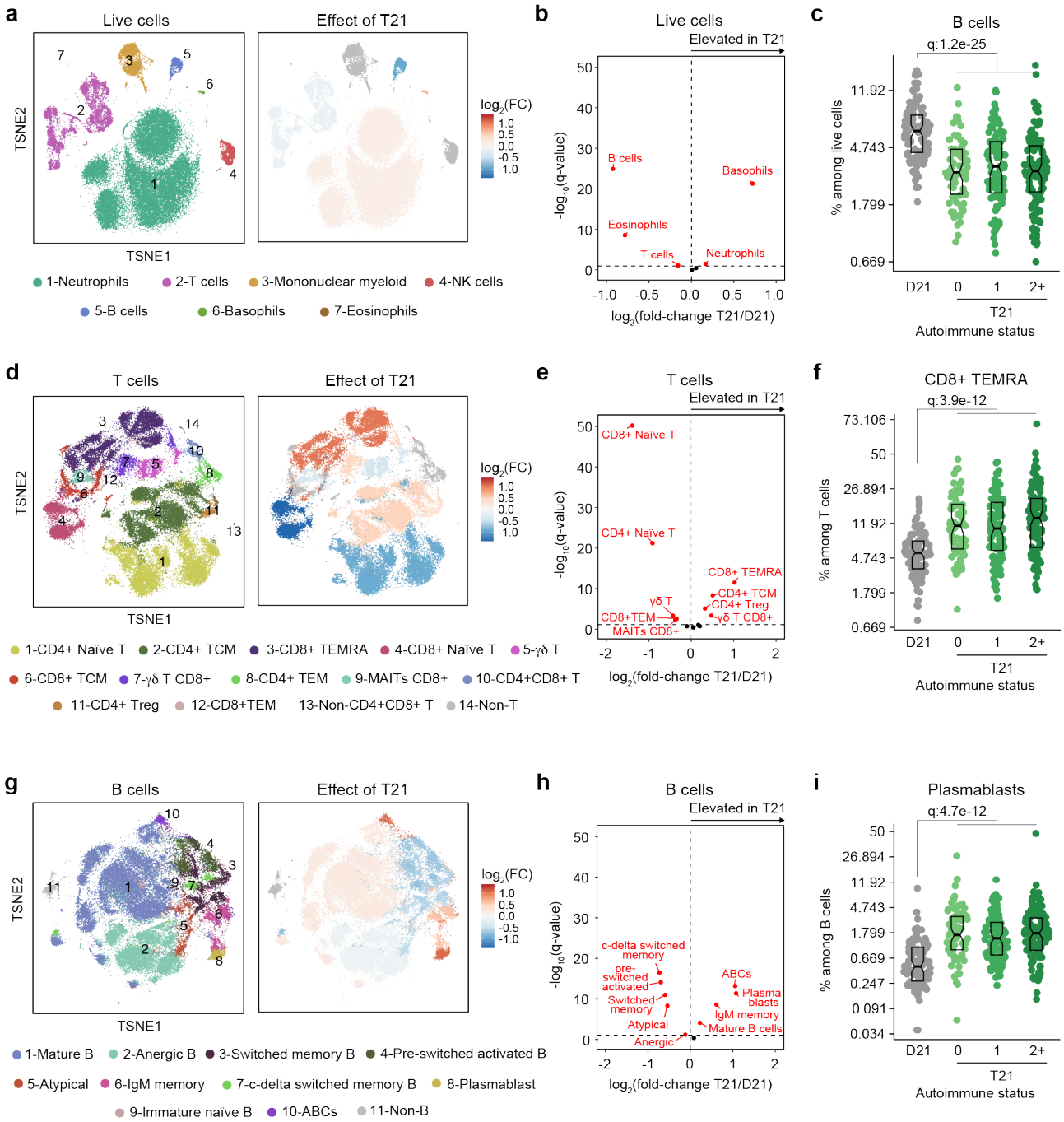

Figure 2. Trisomy 21 causes global immune remodeling regardless of clinically evident autoimmunity. a, t-distributed Stochastic Neighbor Embedding (t-SNE) plot displaying major immune populations identified by FlowSOM analysis of mass cytometry data for all live cells (left) and color coded by significant impact of T21 (beta regression q<0.1) on their relative frequency (right). Red indicates increased frequency and blue indicates decreased frequency among research participants with T21 (n=292) versus euploid controls (D21, n=96). **b**, Volcano plot showing the results of beta regression

251 analysis of major immune cell populations among all live cells in research participants with T21 (n=292)
252 versus euploid controls (D21, n=96). The dashed horizontal line indicates a significance threshold of
253 10% FDR (q<0.1) after Benjamini-Hochberg correction for multiple testing. **c**, Frequencies of B cells
254 among all live cells in euploid controls (D21, n=96) versus individuals with T21 and history of 0 (n=69),
255 1 (n=102) or 2+ (n=121) autoimmune/inflammatory conditions. Data is displayed as modified sina plots
256 with boxes indicating quartiles. **d-f**, Description as in a-c, but for subsets of T cells. **g-i**, Description as
257 in a-c, but for subsets of B cells.
258

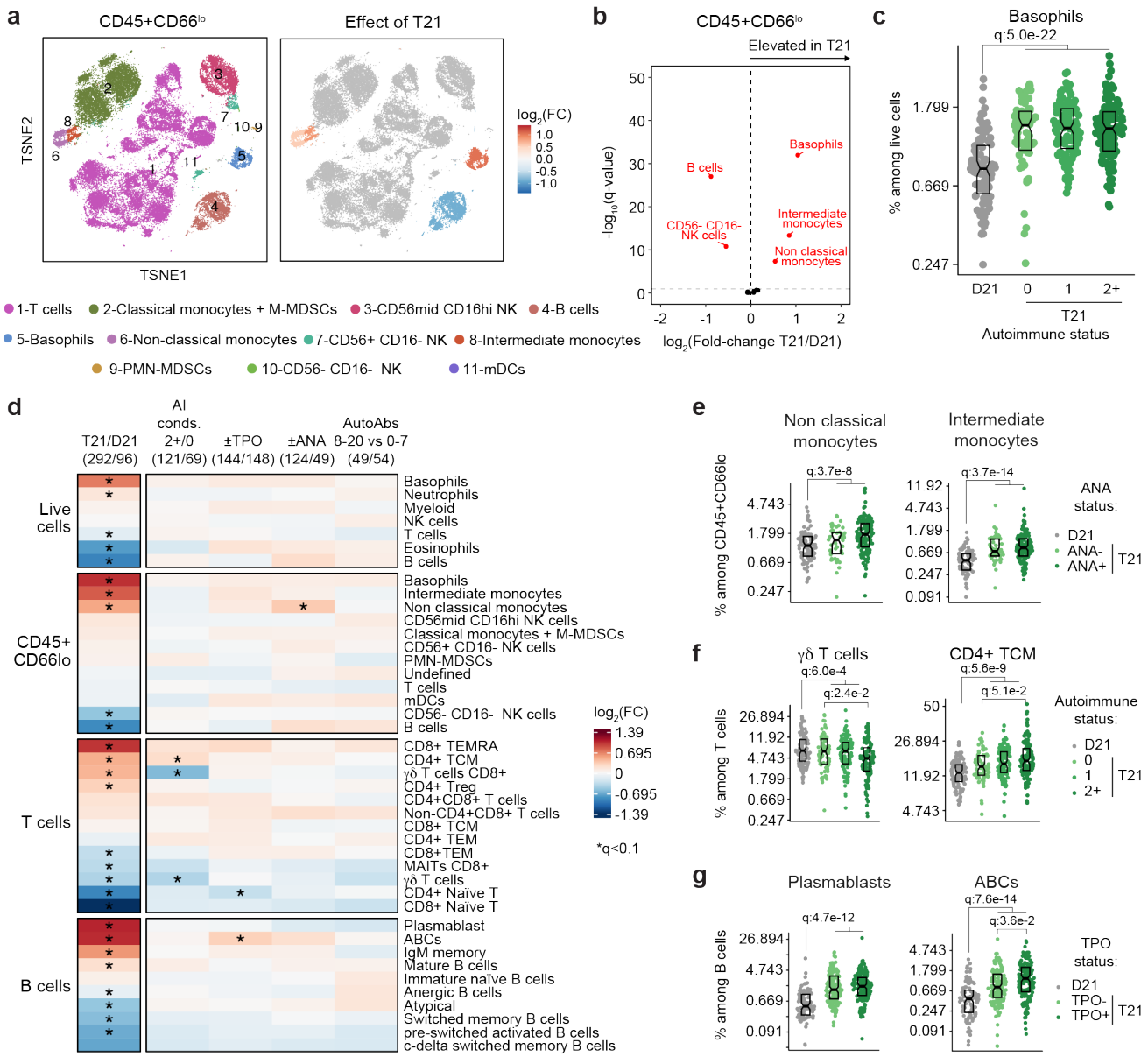

Figure 2 – figure supplement 1. Consistent remodeling of the peripheral immune system in Down syndrome. a, t-distributed Stochastic Neighbor Embedding (t-SNE) plot displaying major immune populations identified by FlowSOM analysis of mass cytometry data for CD45+ CD66^{lo} non-granulocytes (left) and color coded by the impact of trisomy 21 (T21) on their relative frequency (right). Red indicates increased frequency and blue indicates decreased frequency among research participants with T21 (n=292) versus euploid controls (D21, n=96). **b**, Volcano plot showing the results of beta regression analysis of immune cell populations among CD45+ CD66^{lo} non-granulocytes from research participants with T21 (n=292) versus euploid controls (D21, n=96). The dashed horizontal line indicates

268 a significance threshold of 10% FDR (q<0.1) after Benjamini-Hochberg correction for multiple testing.
269 **c**, Frequencies of basophils among all live cells in euploid controls (D21, n=96) versus individuals with
270 T21 and history of 0 (n=44), 1 (n=71) or 2+ (n=88) autoimmune/inflammatory conditions. Data is
271 displayed as modified sina plots with boxes indicating quartiles. **d**, Heatmap summarizing the results of
272 beta regression testing for differences in frequencies of indicated immune cell populations among all
273 live cells, CD45+ CD66^{lo} non-granulocytes, T cells, and B cells by T21 (n=292) versus D21 (n=96)
274 status, or by different subgroups within the T21 cohort: 2+ (n=88) versus 0 (n=44)
275 autoimmune/inflammatory conditions; TPO+ (n=144) versus TPO- (n=148); ANA+ (n=124) versus
276 ANA- (n=49); or positivity for 8-20 (n=49) versus 0-7 (n=54) autoantibodies elevated in DS. Asterisks
277 indicate significance after Benjamini-Hochberg correction for multiple testing (q<0.1, 10% FDR). **e-g**,
278 Representative examples of immune cell populations from d, showing effects of ANA positivity (e),
279 number of autoimmune conditions (f), and TPO status (g). Data are presented as modified sina plots
280 with boxes indicating quartiles, with q-values indicating beta regression significance after Benjamini-
281 Hochberg correction for multiple testing.
282

283 **Trisomy 21 causes hypercytokinemia from an early age independent of autoimmunity status.**

284 It is well established that individuals with DS display elevated levels of many inflammatory markers,
285 including several interleukins, cytokines, and chemokines known to drive autoimmune conditions, such
286 as IL-6 and TNF-α[18,28,42,45]. However, the interplay between hypercytokinemia, individual elevated
287 cytokines, and development of autoimmune conditions in DS remains to be elucidated. Therefore, we
288 analyzed data available from the HTP cohort for 54 inflammatory markers in plasma samples from 346
289 individuals with DS versus 131 euploid controls and cross-referenced these data with the presence of
290 autoimmune conditions and autoantibodies. These efforts confirmed the notion of profound
291 hypercytokinemia in DS[18,28,42,45], with significant elevation of multiple acute phase proteins (e.g. CRP,
292 SAA, IL1RA), pro-inflammatory cytokines (TSLP, IL-17C, IL-22, IL-17D, IL-9, IL-6, TNF-α) and
293 chemokines (IP-10, MIP-3a, MIP-1a, MCP-1, MCP-4, Eotaxin), as well as growth factors associated with
294 inflammation and wound healing (FGF, PlGF, VEGF-A) (**Figure 3a**). However, when evaluating for
295 differences within the DS cohort based on various metrics of autoimmunity, we did not observe important
296 differences based on number of autoimmune/inflammatory conditions, ANA or TPO positivity status, or
297 number of other autoantibodies (**Figure 3a**). For example, CRP, IL-6, and TNF-α are equally elevated
298 across all these subgroups (**Figure 3b-d, Figure 3 - figure supplement 1a**).

299 Previous studies have reported signs of early immunosenescence and inflammaging in DS, including
300 accelerated progression of immune lineages toward terminally differentiated states, early thymic atrophy,
301 and elevated levels of pro-inflammatory markers associated with age in the typical population[25,27,46,47].
302 However, the extent to which the inflammatory profile of DS represents accelerated ageing versus other
303 processes remains ill-defined. To address this, we first identified age-associated changes in immune
304 markers within the euploid and DS cohorts separately (**Figure 3 - figure supplement 1b-c**). This exercise
305 identified multiple immune markers that were up- or down-regulated with age, with an overall conserved
306 pattern of age trajectories in both groups (**Figure 3 - figure supplement 1c**). For example, increased age
307 is associated with increased CRP levels and decreased IL-17B levels in both cohorts (**Figure 3 - figure**

308 **supplement 1d**). We then compared the effects of age versus T21 status on cytokine levels in the DS
309 cohort, which identified many inflammatory factors elevated in DS across the lifespan that do not display
310 a significant increase with age, such as IL-9 and IL-17C, or that increase with age only in the DS cohort,
311 such as IP-10 (**Figure 3e-f, Figure 3 - figure supplement 1e**).

312 Altogether, these results indicate that T21 induces a constitutive hypercytokinemia from early
313 childhood, with only a fraction of these inflammatory changes being exacerbated with age.

314

315

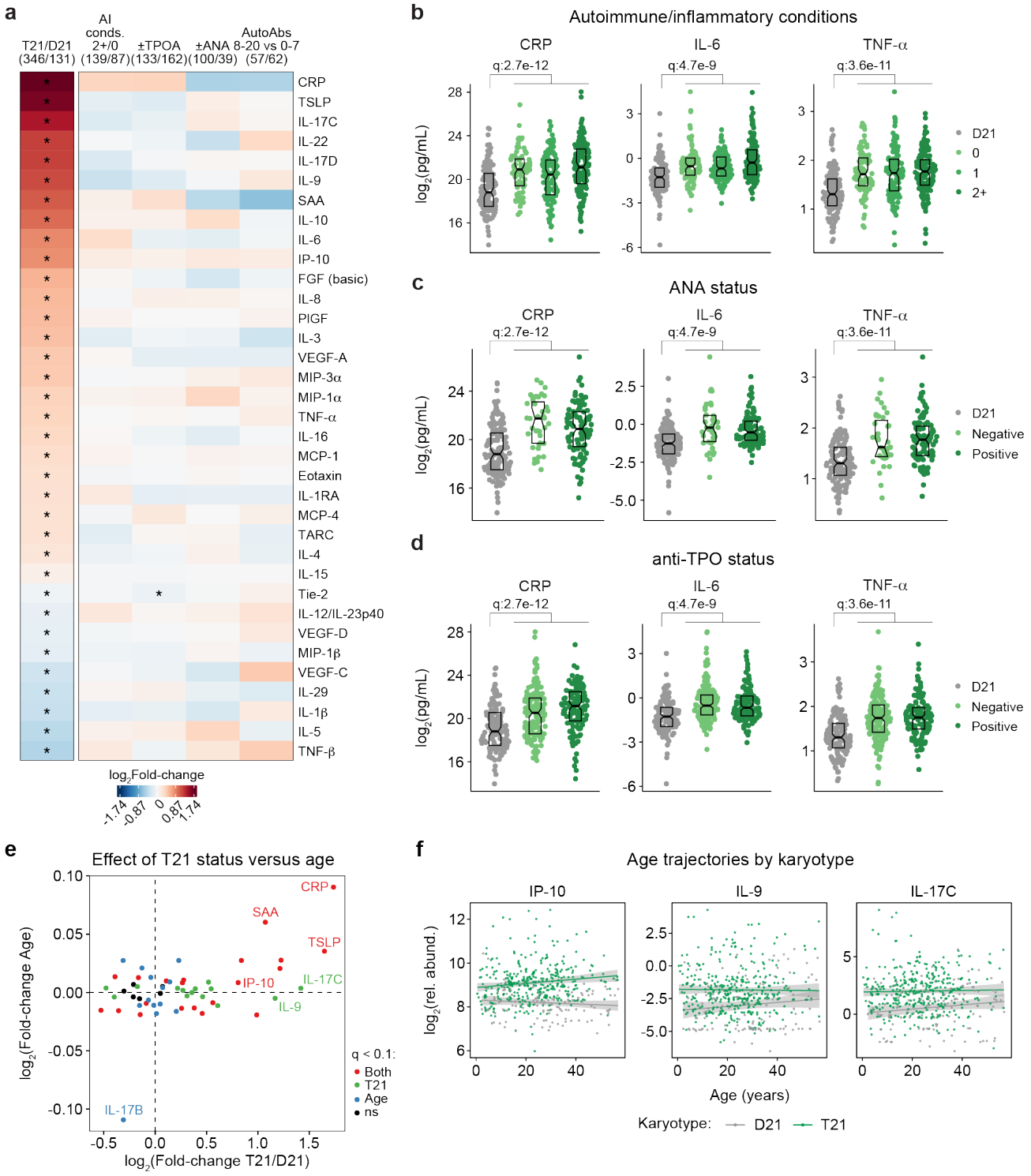

Figure 3. Trisomy 21 causes constitutive hypercytokinemia independent of autoimmunity status from an early age. a, Heatmap displaying $\log_2$-transformed fold-changes for plasma immune markers with significant differences in trisomy 21 (T21, n=346) versus euploid (D21, n=131), and between different subgroups within the T21 cohort: history of 2+ (n=139) versus 0 (n=87)

321 autoimmune/inflammatory conditions (AI conds.); TPO+ (n=133) versus TPO- (n=162); ANA+ (n=100)
322 versus ANA- (n=39); or positivity for 8-20 (n=57) versus 0-7 (n=62) autoantibodies (AutoAbs) elevated
323 in DS. Asterisks indicate linear regression significance after Benjamini-Hochberg correction for multiple
324 testing (q<0.1, 10% FDR). **b-d**, Comparison of CRP, IL-6 and TNF-α levels in euploid controls (D21,
325 n=131) versus subsets of individuals with T21 based on number of autoimmune/inflammatory
326 conditions (**b**), ANA positivity (**c**) or TPO positivity (**d**). Data are presented as modified sina plots with
327 boxes indicating quartiles. Samples sizes as in a. q-values indicate linear regression significance after
328 Benjamini-Hochberg correction for multiple testing. **e**, Scatter plot comparing the effect of T21
329 karyotype versus the effect of age in individuals with T21 (n=54 immune markers in 346 individuals
330 with T21), highlighting immune markers that are significantly different by T21 status, age, or both. ns:
331 not significantly different by T21 status or age. **f**, Scatter plots for example immune markers that are
332 significantly elevated in T21, but which are either not elevated with age in the euploid (D21) cohort (i.e.,
333 IP-10), or in either the T21 (n=346) or D21 (n=131) cohorts. Lines represent least-squares linear fits
334 with 95% confidence intervals in grey.
335

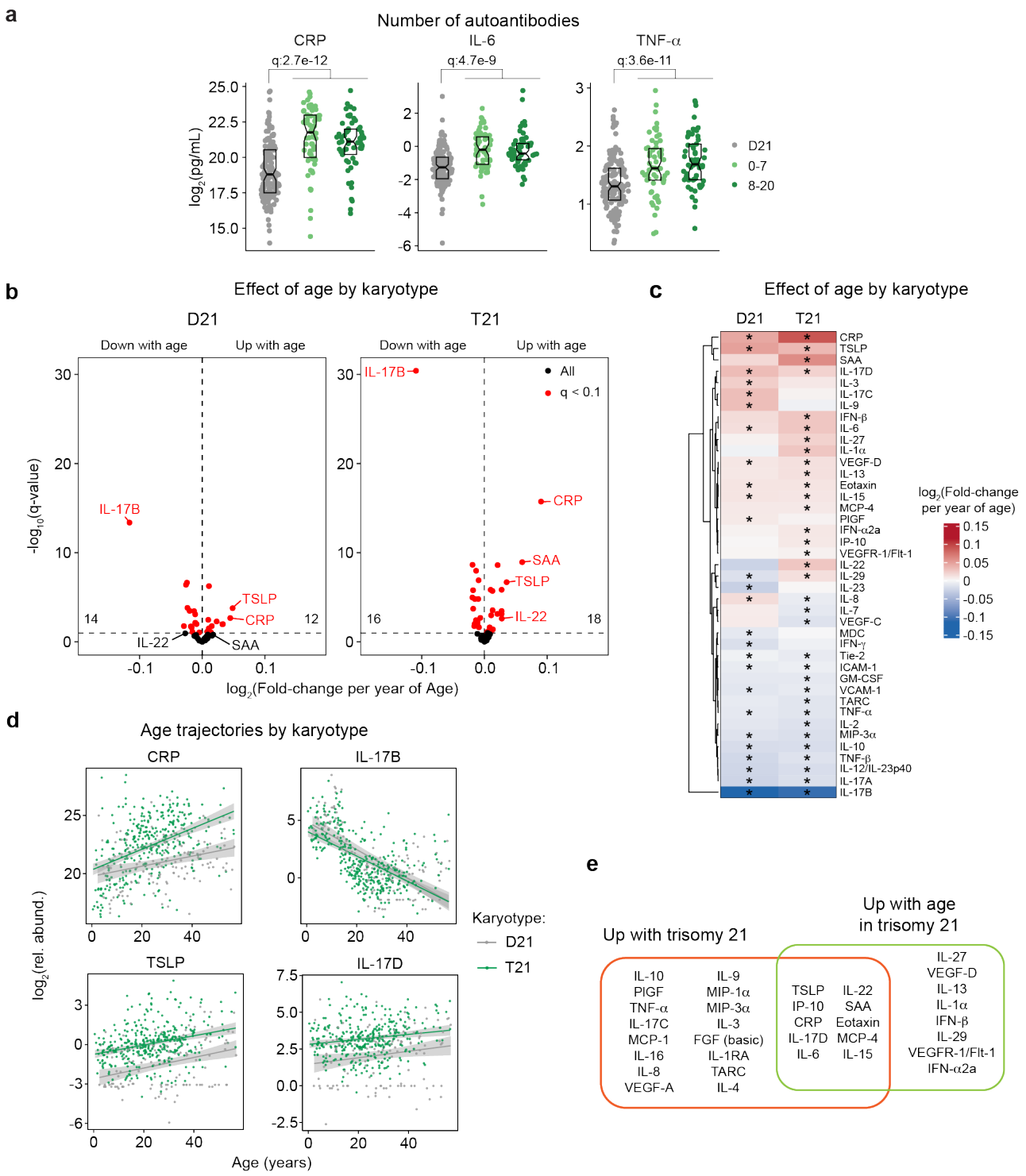

Figure 3 – figure supplement 1. Consistent hypercytokinemia from an early age in Down syndrome. a, Comparison of CRP, IL-6, and TNF-α levels in euploid controls (D21, n=131) versus subsets of individuals with T21 based on number of autoantibodies commonly elevated in Down syndrome: 0-7 autoantibodies (n=62) versus 8-20 autoantibodies (n=57). Data are presented as modified

341 sina plots with boxes indicating quartiles. q-values indicate linear regression significance after
342 Benjamini-Hochberg correction for multiple testing. **b**, Volcano plots presenting the results of linear
343 regression testing for association between age and the levels of 54 immune markers in the plasma of
344 euploid controls (left, D21, n=131) and individuals with trisomy 21 (right, T21, n=346) enrolled in the
345 Human Trisome Project (HTP) study. Horizontal dashed lines indicate a significance threshold of 10%
346 FDR ($q<0.1$) after Benjamini-Hochberg correction for multiple testing. **c**, Heatmap comparing the effect
347 of age on levels of immune markers in D21 and T21. Heatmap color scale represents log2-transformed
348 mean fold-change per year of age; asterisks indicate significance ($q < 0.1$) for linear regression testing.
349 **d**, Scatter plots showing the age trajectories of select immune markers in D21 versus T21. Sample sizes
350 as in c. Lines represent least squares linear fits with shaded areas indicating 95% confidence interval. **e**,
351 Diagram representing the overlap between immune markers elevated in T21 versus D21 and those
352 elevated with age in T21.

353

354 **A clinical trial for JAK inhibition in Down syndrome.**

355 Several lines of evidence support the notion that IFN hyperactivity and downstream JAK/STAT
356 signaling are key drivers of immune dysregulation in DS[15-19,22,24,42,48]. In mouse models of DS, both
357 normalization of *IFNR* gene copy number and pharmacologic JAK1 inhibition rescue their lethal immune
358 hypersensitivity phenotypes[22,48]. Furthermore, we recently demonstrated that IFN transcriptional scores
359 derived from peripheral immune cells correlate significantly with the degree of immune remodeling and
360 hypercytokinemia in DS[42], and we and others have reported the safe use of JAK inhibitors for treatment
361 of diverse immune conditions in DS, including alopecia areata[49], psoriatic arthritis[50] and hemophagocytic
362 lymphohistocytosis[51] through small case series. Encouraged by these results, we launched a clinical trial
363 to assess the safety and efficacy of the JAK inhibitor tofacitinib (Xeljanz, Pfizer) in DS, using moderate-
364 to-severe autoimmune/inflammatory skin conditions as a qualifying criterion (NCT04246372). This trial
365 is a single-site, open-label, Phase II clinical trial enrolling individuals with DS between the ages of 12 and
366 50 years old affected by alopecia areata, hidradenitis suppurativa, psoriasis, atopic dermatitis, or vitiligo
367 (see qualifying disease scores in **Supplementary file 3**). After screening, qualifying participants are
368 prescribed 5 mg of tofacitinib twice daily for 16 weeks, with an optional extension to 40 weeks (**Figure**
369 **4a**, see **Materials and Methods**). After enrollment and assessments at a baseline visit, participants attend
370 five safety monitoring visits during the main 16-week trial period. The recruitment goal for this trial is 40
371 participants who complete 16 weeks of tofacitinib treatment, with an IRB-approved qualitative interim
372 analysis triggered when the first 10 participants completed the main 16-week trial (**Figure 4b**). Among
373 the first 13 participants enrolled, one participant withdrew shortly after enrollment, one was excluded from
374 analyses due to medication non-compliance (i.e., >15% missed doses), and one participant had not yet
375 completed the trial at the time of the interim analysis (**Figure 4b**). Demographic characteristics of the 10
376 participants included in the interim analysis are shared in **Supplementary file 3**. Baseline qualifying
377 conditions of the 10 participants included in the interim analysis were alopecia areata (n=6), hidradenitis
378 suppurativa (n=3), and psoriasis (n=1) (open circles in **Figure 4c**). Two participants presented with

379 concurrent atopic dermatitis, two with concurrent vitiligo, and two with concurrent hidradenitis
380 suppurativa, albeit below the severity required to be the qualifying conditions (see closed circles in **Figure**
381 **4c**). In addition, seven participants had AITD/TPO+ and three had a celiac disease diagnosis (**Figure 4c**).
382

383 **Tofacitinib is well tolerated in Down syndrome.**

384 Analysis of adverse events (AEs) recorded for the 10 first participants over 16 weeks did not identify
385 any AEs considered definitely related to tofacitinib treatment or classified as severe. Several AEs were
386 annotated as 'possibly related' to treatment (**Figure 4d, Supplementary file 4**). Five episodes of upper
387 respiratory infections (URIs) affecting five different participants were observed. Based on the safety data
388 for tofacitinib in the general population[52], all episodes of URIs were annotated as possibly related to
389 treatment. Participant AA2 developed occasional cough and rhinorrhea that resolved with over-the-
390 counter medication. Two other participants reported transient rhinorrhea (AA3, AA5). Participant AA4
391 developed a nasal congestion, with chest pain and a productive cough. This participant tested negative for
392 SARS-Co-V2, Flu A-B, and RSV. Tofacitinib was not paused during this episode, and symptoms resolved
393 with over-the-counter medication. Participant HS2 experienced a sore throat with middle ear inflammation
394 that resolved with over-the-counter treatment. This participant also presented with folliculitis, which
395 resolved with antibiotic treatment. Participant HS1 experienced a short transient elevation (<3 days) in
396 creatine phosphokinase (CPK) that resolved spontaneously, and rash acneiform. Participant Ps1
397 experienced a transient and asymptomatic decrease in white blood cell (WBC) counts that resolved by the
398 end of the trial.

399 Overall**,** tofacitinib treatment was not discontinued for any of the 10 participants over the 16-week
400 study period, and seven participants eventually obtained off-label prescriptions after completing the trial
401 and are currently taking the medicine. Based on these interim results, recruitment resumed and is ongoing.
402

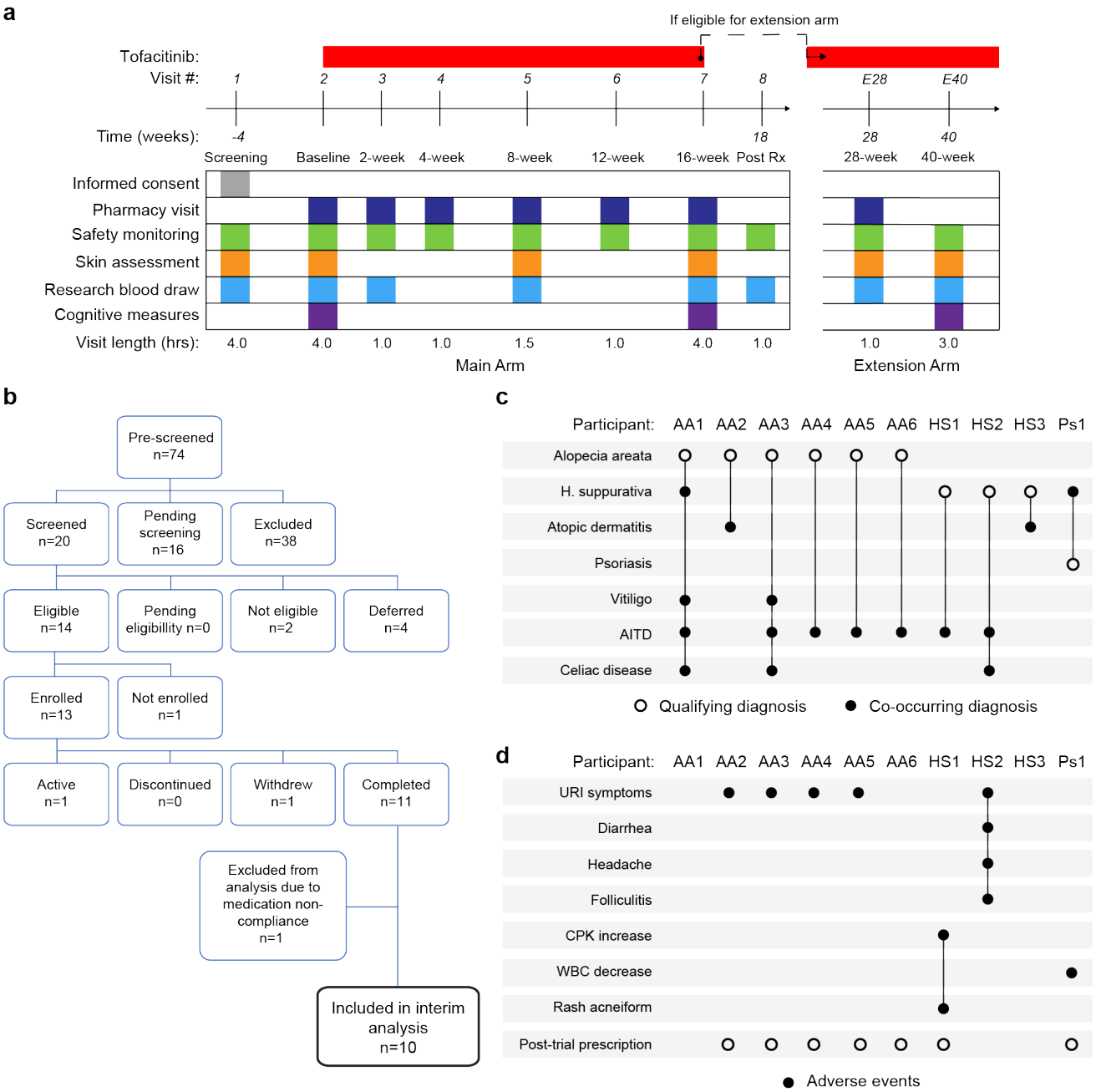

Figure 4. Clinical trial for JAK inhibition in Down syndrome. a, Schedule of activities for clinical trial of JAK inhibition in Down syndrome (NCT04246372). **b,** Consort chart for first 13 participants enrolled in the clinical trial. **c,** Upset plot displaying the qualifying and co-occurring autoimmune/inflammatory conditions for the 10 participants included in the interim analysis. **d,** Upset plots summarizing the adverse events annotated for the first 10 participants over a 16-week treatment period.

410 **Tofacitinib improves diverse autoimmune/inflammatory skin conditions in Down syndrome**.

411 In the clinical trial, skin pathology is monitored using global metrics of skin health, including the
412 Investigator's Global Assessment (IGA) and the Dermatology Life Quality Index (DLQI), as well as
413 disease-specific scores, such as the severity of alopecia tool (SALT), the psoriasis area and severity index
414 (PASI), or the eczema area and severity index (EASI) (see **Materials and Methods, Supplementary file**
415 **5**. The interim analysis showed that seven of the ten participants had an improvement in the IGA score
416 and eight of the ten reported some improvement on their life quality related to their skin condition as
417 measured by the DLQI (**Figure 5a-b**). The most striking effects were observed for alopecia areata (**Figure**
418 **5c-d, Figure 5 – figure supplement 1a**). Five of six participants with alopecia areata showed scalp hair
419 regrowth, with the exception being a male participant (AA1) with history of alopecia totalis for 20+ years
420 who only showed facial hair and eyelash re-growth. One participant presented with psoriasis due to
421 psoriatic arthritis and experienced an almost complete remission of psoriatic arthritis symptoms (Ps1,
422 **Figure 5 – figure supplement 1b-c**). For the two participants that presented with atopic dermatitis, the
423 clinical manifestations were markedly reduced during tofacitinib treatment (**Figure 5e-f**). A total of five
424 participants were affected by HS, three of them as the qualifying condition (HS1-3). No clear trend was
425 seen in the Modified Sartorius Scale (MSS) score used to monitor HS (**Figure 5 – figure supplement 1d-**
426 **e**).

427 Altogether, these results indicate that JAK inhibition could provide therapeutic benefit for several
428 autoimmune/inflammatory skin conditions more common in DS.

429

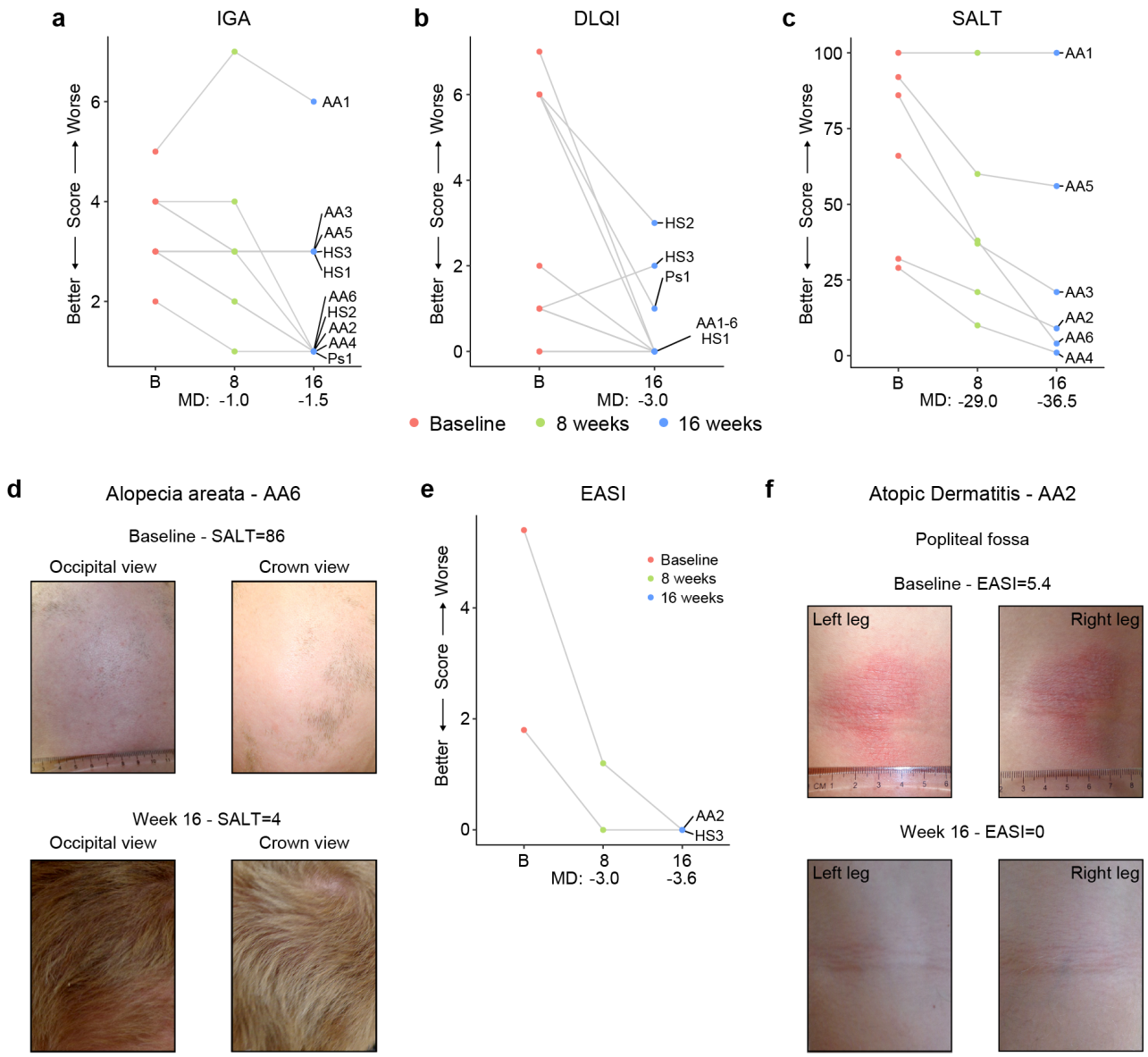

Figure 5. Tofacitinib improves diverse immune skin pathologies in Down syndrome. a-b, Investigator global assessment (IGA) scores (a) and Dermatological Life Quality Index (DLQI) scores (b) for the first 10 participants at baseline visit (B), mid-point (8 weeks) and endpoint (16 weeks) visits. MD: median difference. **c,** Severity of Alopecia Tool (SALT) scores for the first seven participants with alopecia areata in the trial. **d,** Images of participant AA6 at baseline versus week 16. **e,** Eczema Area and Severity Index (EASI) scores for two participants with mild atopic dermatitis. **f,** Images of participant AA2 showing improvement in atopic dermatitis upon tofacitinib treatment. p values not shown as per interim analysis plan.

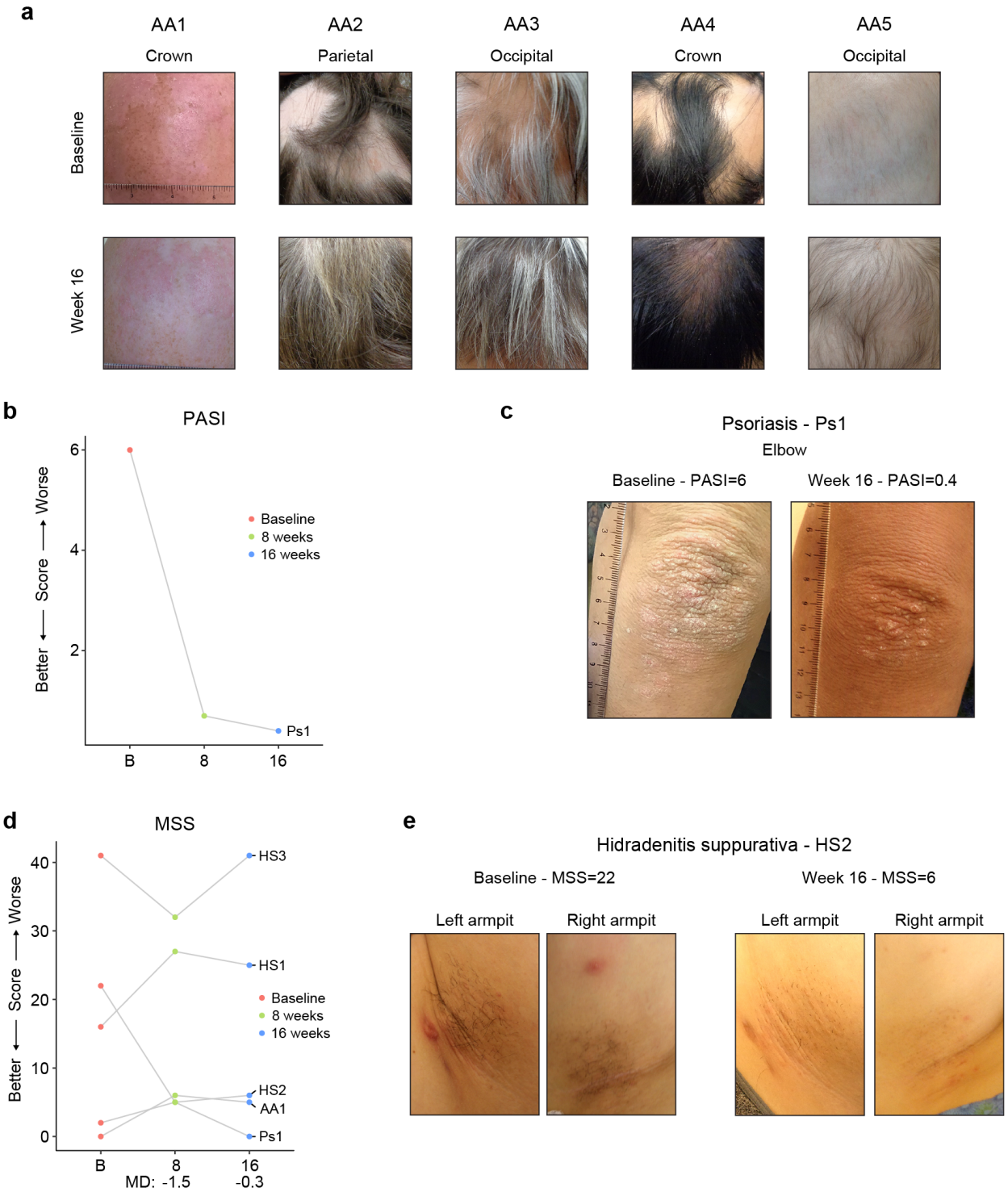

Figure 5 – figure supplement 1. Tofacitinib improves diverse skin pathologies in Down syndrome. **a,** Images of five participants with alopecia areata at baseline and after 16 weeks of tofacitinib treatment. **b-c**, Psoriasis Area and Severity Index score (b) and images (c) for participant with psoriatic arthritis. **d,** Modified Sartorius Scale (MSS) scores for five participants with hidradenitis suppurativa (HS). MD:

444 median difference. **e**, Images for participant affected by HS at baseline and 16-week endpoint visit. p

445 values not shown as per interim analysis plan.

446

447 **Tofacitinib normalizes IFN scores and decreases pathogenic cytokines and autoantibodies.**

448 It is well demonstrated that individuals with DS display elevated IFN signaling across multiple
449 immune and non-immune cell types[15-17,19]. Using an IFN transcriptional score composed of 16 interferon-
450 stimulated genes (ISGs)[53] measured via bulk RNA sequencing of peripheral blood RNA, individuals with
451 DS in the HTP cohort study show a significant increase in these scores[48] (**Figure 6a**). Reduction of IFN
452 scores is designated as a primary endpoint in the trial. At baseline, clinical trial participants show IFN
453 scores within the typical range for DS, but values are decreased at 2, 8, and 16 weeks of tofacitinib
454 treatment (**Figure 6a, Supplementary file 6**). Time course analysis revealed that most participants show
455 a decrease in IFN scores as soon as two weeks of treatment which is sustained over time, with two clear
456 exceptions (**Figure 6 – figure supplement 1a**). At the 8-week study midpoint, 9 of 10 participants had
457 decreased IFN scores relative to baseline, except participant AA2 who reported a COVID-19 vaccination
458 three days prior to the visit and was pausing tofacitinib at the time of the blood draw (**Figure 6 – figure**
459 **supplement 1a**). At the 16-week time point, nine of ten participants had decreased IFN scores, with the
460 exception being AA4, who developed an URI in the week prior to the blood draw (**Figure 6 – figure**
461 **supplement 1a**). Therefore, although all participants displayed decreased IFN scores at one or more time
462 points during the treatment, IFN scores could be sensitive to immune triggers. Analysis of individual ISGs
463 composing the IFN score revealed that whereas many ISGs elevated in DS display reduced expression
464 upon tofacitinib treatment (e.g., *RSAD2*, *IFI44L*), others do not (e.g., *BPGM*) (**Figure 6b, Figure 6 –**
465 **figure supplement 1b**). To investigate this further, we defined the impact of tofacitinib on all 136 ISGs
466 significantly elevated in DS that are not encoded on chr21[42] (**Figure 6c**). Collectively, ISGs as a group
467 are significantly downregulated upon tofacitinib treatment, but the effect is not uniform across all ISGs
468 (**Figure 6c**), indicating that JAK1/3 inhibition does not reduce all IFN signaling elevated in DS, which
469 could be explained by the fact that the IFN pathways also employ JAK2 for signal transduction[54,55]. Global
470 analysis of transcriptome changes revealed that tofacitinib treatment reverses the dysregulation of many
471 gene signatures observed in DS, effectively attenuating many pro-inflammatory signatures beyond IFN

472 gamma and alpha responses, such as Inflammatory Response, TNF-α signaling via NFkB, IL-2 STAT5
473 signaling, and IL-6 JAK STAT3 signaling (**Figure 6 – figure supplement 1c**). Tofacitinib also reversed
474 elevation of genes involved in Oxidative Phosphorylation and dampened downregulation of gene sets
475 involved in Wnt/Beta Catenin and Hedgehog Signaling (**Figure 6 – figure supplement 1c-d**). Conversely,
476 tofacitinib did not rescue elevation of genes involved in Heme Metabolism or Mitotic Spindle (**Figure 6**
477 **– figure supplement 1c-d**), suggesting that these transcriptome changes are not tied to the inflammatory
478 profile of DS.

479 A secondary endpoint in the trial is decrease of peripheral inflammatory markers as defined by a
480 composite cytokine score derived from measurements of TNF-α, IL-6, CRP, and IP-10, and which is
481 significantly increased in participants with DS in the HTP study (**Figure 6d**). At baseline, clinical trial
482 participants show cytokine scores within the range observed for DS, but these values decrease at 2, 8 and
483 16 weeks relative to baseline (**Figure 6d-e, Figure 6 – figure supplement 1e**). The decreases in TNF-α
484 and IL-6 observed upon tofacitinib treatment indicates that elevation of these potent inflammatory
485 cytokines requires sustained JAK/STAT signaling in DS (**Figure 6e**). As for the IFN scores assessment,
486 time course analysis revealed that most participants show decreases in cytokine scores within two weeks
487 of treatment that are sustained over time, again with the exception of AA2 at week 8 and AA4 at week 16.
488 This reveals a correspondence between RNA-based transcriptional IFN scores and circulating levels of
489 these cytokines in plasma, while also illustrating that both metrics may remain sensitive to immune
490 triggers (**Figure 6 – figure supplement 1f-g**).

491 One tertiary endpoint of the trial investigates the impact of tofacitinib treatment on levels of
492 autoantibodies and markers employed to diagnose AITD [e.g., anti-TPO, anti-TG, anti-thyroid stimulating
493 hormone receptor (TSHR)] and celiac disease [e.g., anti-tissue transglutaminase (tTG), anti-deamidated
494 gliadin peptide (DGP)]. Seven of the 10 participants presented at baseline with anti-TPO levels above the
495 upper limit of normal (ULN, 60U/mL), and all seven experienced a decrease in these auto-antibodies at 8
496 weeks and 16 weeks relative to baseline (**Figure 6f**). In fact, for one participant (HS1) the levels decreased

497 below the ULN while on the trial. All seven of these participants had a history of thyroid disease (**Figure**
498 **4c**), which was being medically managed and/or clinically monitored with acceptable TSH and T4 values.
499 Additionally, three of these seven participants also had anti-TG levels above the ULN (4 IU/mL) and all
500 three showed a decrease from baseline levels while on tofacitinib at both 8 and 16 weeks, with one
501 participant (AA6) falling below the ULN upon treatment (**Figure 6f**). Three participants also had anti-
502 TSHr levels above the ULN, but no clear changes were observed upon treatment (**Supplementary file 5**).
503 None of the 10 participants displayed anti-tTG or anti-DGP levels detected above ULN at screening.
504 Altogether, these results indicate that tofacitinib treatment decreases IFN scores, levels of key
505 pathogenic cytokines, and key autoantibodies involved in AITD. Importantly, tofacitinib treatment lowers
506 IFN scores and cytokine levels to within the range observed in the general population, not below,
507 indicating that this immunomodulatory strategy can provide therapeutic benefit in DS without overt
508 immune suppression.
509

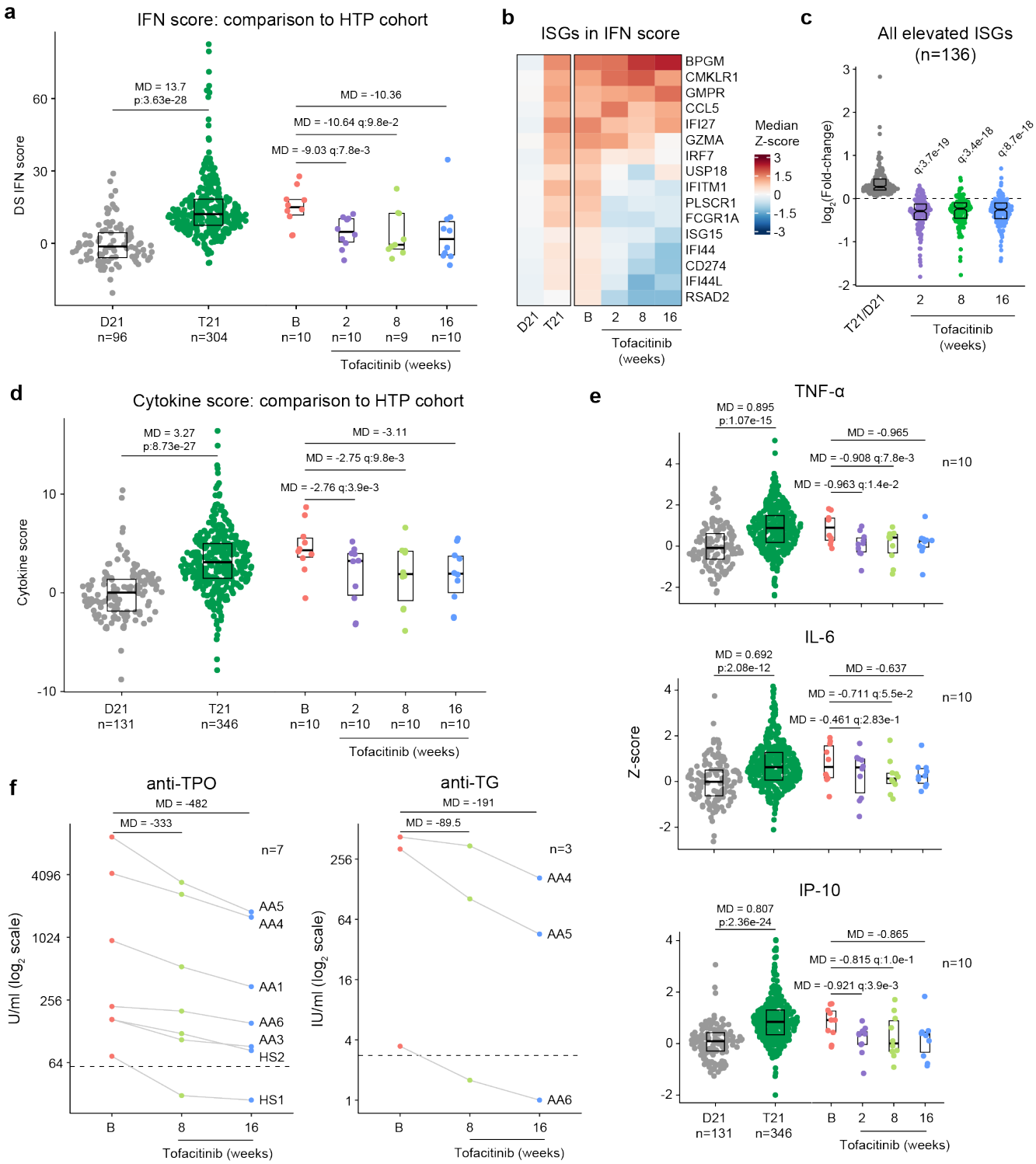

510

511 **Figure 6. Tofacitinib reduces IFN scores, hypercytokinemia, and pathogenic autoantibodies in**
512 **Down syndrome. a,** Comparison of interferon (IFN) transcriptional scores derived from whole blood
513 transcriptome data for research participants in the Human Trisome Project (HTP) cohort study by
514 karyotype status (D21, grey; T21, green) and the clinical trial cohort at baseline (B), and weeks 2, 8 and

515 16 of tofacitinib treatment. Data are represented as modified sina plots with boxes indicating quartiles.
516 Sample sizes are indicated below the x-axis. Horizontal bars indicate comparisons between groups with
517 median differences (MD) with p-values from Mann-Whitney U-tests (HTP cohort) or q-values from paired
518 Wilcox tests (clinical trial). q value for the 16-week endpoint is not shown as per interim analysis plan. **b,**
519 Heatmap displaying median z-scores for the indicated groups (as in a) for the 16 interferon-stimulated
520 genes (ISGs) used to calculate IFN scores. **c,** Analysis of fold changes for 136 ISGs not encoded on chr21
521 that are significantly elevated in Down syndrome (T21 versus D21) at 2, 8 and 16 weeks of tofacitinib
522 treatment relative to baseline. Sample sizes as in a. q-values above each group indicate significance of
523 Mann-Whitney U-tests against log2-transformed fold-change of 0 (no-chance), after Benjamini-Hochberg
524 correction for multiple testing. **d,** Comparison of cytokine score distributions for the HTP cohort by
525 karyotype status (D21, T21) versus the clinical trial cohort at baseline (B) and 2, 8 and 16 weeks of
526 tofacitinib treatment. Data are represented as modified sina plots with boxes indicating quartiles. Sample
527 sizes are indicated below the x-axis. Horizontal bars indicate comparisons between groups with median
528 differences (MD) with p-values from Mann-Whitney U-tests (HTP cohort) and q-values from paired
529 Wilcox tests (clinical trial). q value for the 16-week endpoint is not shown as per interim analysis plan. **e,**
530 Comparison of plasma levels of cytokines in the HTP cohort by karyotype status (D21, T21) and the
531 clinical trial cohort at baseline (B) versus 2, 8 and 16 weeks of tofacitinib treatment. Data are represented
532 as modified sina plots with boxes indicating quartiles. Sample sizes are indicated below x-axis. Horizontal
533 bars indicate comparisons between groups with median differences (MD) with p-values from Mann-
534 Whitney U-tests (HTP cohort) and q values from paired Wilcox tests (clinical trial). q value for the 16-
535 week endpoint is not shown as per interim analysis plan. **f,** Plots showing levels of autoantibodies against
536 thyroid peroxidase (TPO) and thyroglobulin (TG) at baseline versus 8 and 16 weeks of tofacitinib
537 treatment. Sample sizes are indicated in each plot.
538

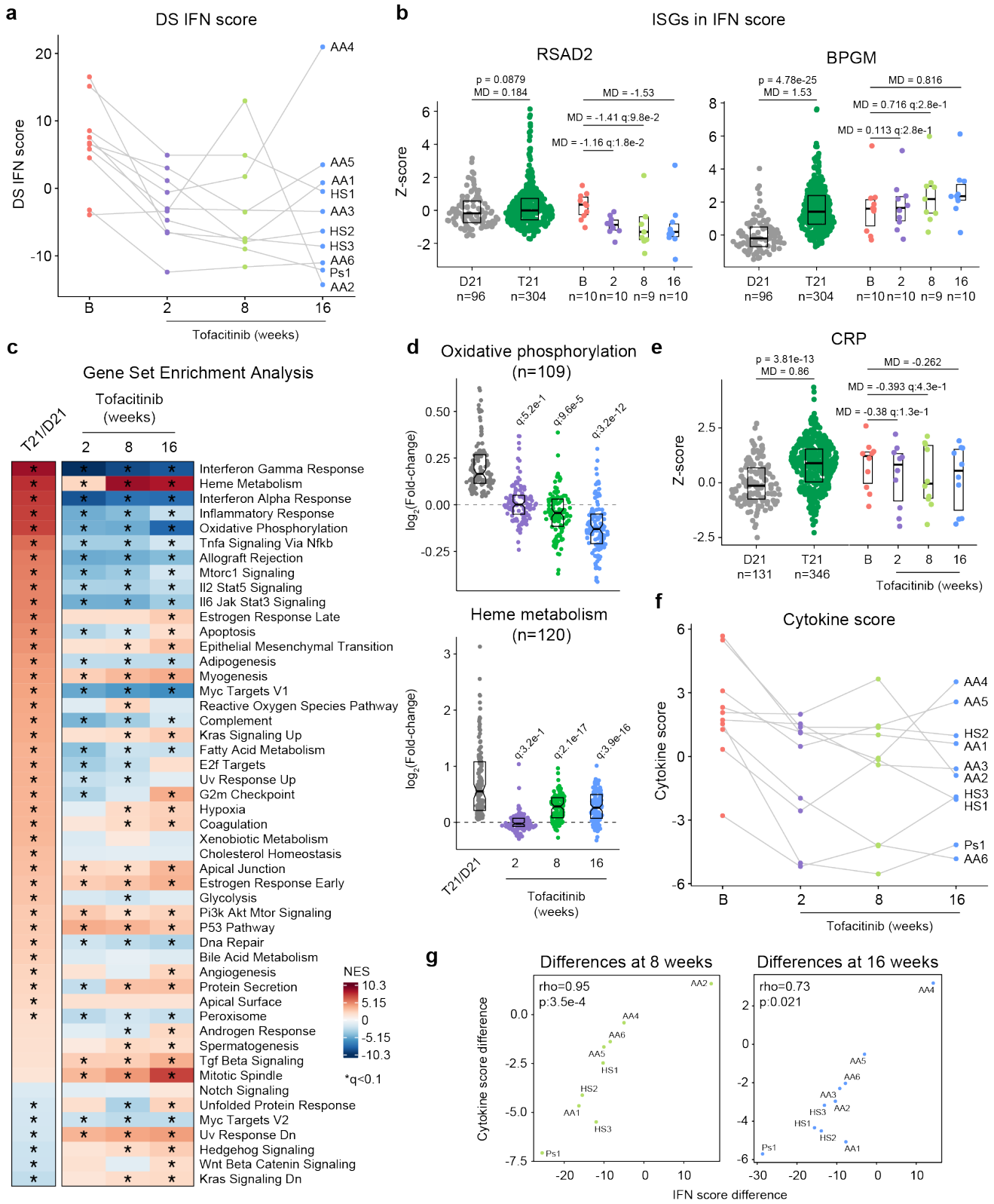

Figure 6 – figure supplement 1. JAK inhibition reduces multiple markers of inflammation and autoimmunity in Down syndrome. a, Plot showing trajectory of IFN scores derived from whole blood transcriptome for 10 clinical trial participants at baseline (B), versus 2, 8 and 16 weeks of tofacitinib

543 treatment. **b**, Comparison of ISG expression in the whole blood transcriptome data from research
544 participants in the Human Trisome Project (HTP) cohort study by karyotype status (D21, grey; T21, green)
545 and the clinical trial cohort at baseline (B), and weeks 2, 8 and 16 of tofacitinib treatment. Data are
546 represented as modified sina plots with boxes indicating quartiles. Sample sizes are indicated below x-
547 axis. Horizontal bars indicate comparisons between groups with median differences (MD) with p-values
548 from Mann-Whitney U-tests (HTP cohort) and q-values from paired Wilcox tests (clinical trial). **c,**
549 Heatmap displaying the results of Gene Set Enrichment Analysis (GSEA) of global transcriptome changes
550 in the whole blood RNA of research participants in the HTP cohort (T21, n=304; D21, n=96) versus the
551 clinical trial cohort at 2 (n=10), 8 (n=9), and 16 weeks (n=10) of tofacitinib treatment relative to baseline
552 (n=10). Asterisks indicate significance after correction by Benjamini-Hochberg method for multiple
553 testing (q<0.1, 10% FDR). NES: normalized enrichment score. **d,** Analysis of fold changes for 109 genes
554 involved in oxidative phosphorylation and 120 genes involved in heme metabolism significantly elevated
555 in Down syndrome (T21 versus D21 in the HTP cohort) versus the clinical trial cohort at 2, 8 and 16
556 weeks of tofacitinib treatment relative to baseline. Sample numbers as in c. **e,** Comparison of CRP levels
557 in the HTP cohort by karyotype status (D21, grey; T21, green) versus the clinical trial cohort at baseline
558 (B) and 2, 8 and 16 weeks of tofacitinib treatment. Data are represented as modified sina plots with boxes
559 indicating quartiles. Sample sizes are indicated below x-axis. Horizontal bars indicate comparisons
560 between groups with median differences (MD) with p-values from Mann-Whitney U-tests (HTP cohort)
561 and q-values from paired Wilcox tests (clinical trial). **f,** Plot showing trajectory of cytokine scores for 10
562 clinical trial participants at baseline (B), versus 2, 8 and 16 weeks of tofacitinib treatment. **g,** Plots showing
563 Spearman correlations between fold changes in IFN scores versus cytokine scores at 8 and 16 weeks of
564 tofacitinib treatment versus baseline. Sample size is n=10.
565

566 **Discussion.**

567 An increasing body of evidence indicates that immune dysregulation contributes to the
568 pathophysiology of DS and that immunomodulatory therapies could provide multidimensional benefits in
569 this population. In mouse models, triplication of four *IFNR* genes contributes to multiple hallmarks of
570 DS[48,56] and JAK inhibition attenuates global dysregulation of gene expression[42] while rescuing key
571 phenotypes, such as lethal immune hypersensitivity[22] and CHDs[24]. The fact that gene signatures of IFN
572 hyperactivity are present in human embryonic tissues with T21[57] and embryonic tissues from mouse
573 models of DS[48,58] indicates that the harmful effects of IFN hyperactivity could start *in utero*, supporting
574 the notion that DS could be understood, in part, as an inborn error of immunity with similarities to
575 monogenic interferonopathies[59].

576 Results presented here demonstrate that T21 causes widespread multi-organ autoimmunity of pediatric
577 onset, with production of autoantibodies targeting every major organ system. These results justify
578 additional efforts to define the key pathogenic autoantibodies in DS beyond those commonly associated
579 with AITD and celiac disease. Our analysis found significant associations between specific autoantibodies
580 and some conditions more common in DS, but the diagnostic value of these observations will require
581 validation efforts in much larger cohorts, which could lead to a personalized medicine approach for the
582 management of autoimmunity in DS. For example, we found autoantibodies associated with various forms
583 of auditory dysfunction (**Figure 1g**), suggesting the possibility of autoimmune hearing loss in DS[60].
584 Elevated levels of anti-TPO in individuals with history of use of ear tubes suggests an interplay between
585 otitis media and endocrine dysfunction in DS[61]. For example, it is possible that recurrent ear infections
586 cause a chronic immune stimulus that lead to eventual breach of tolerance in this autoimmunity-prone
587 population, even perhaps through epitope mimicry[62]. Antibodies targeting MUSK, which we found to be
588 elevated in DS and associated with co-occurring neurological phenotypes (**Figure 1g-h**), have been linked
589 to development of myasthenia gravis, a chronic autoimmune neuromuscular disease that causes weakness
590 in the skeletal muscles[63]. Whether MUSK antibodies associate with similar phenotypes in DS will require

591 further investigation. Elevation of SRP68 autoantibodies in DS (**Figure 1d,f**), which are common in
592 necrotizing myopathies with cardiovascular involvement[40], suggests a potential autoimmune basis for
593 musculoskeletal and cardiovascular complications in DS, which also warrants additional research.

594 We observed constitutive global immune remodeling and hypercytokinemia regardless of reported
595 diagnoses of autoimmune disease or measurable autoantibody production from an early age, indicative of
596 an autoimmunity-prone state throughout the lifespan. Therefore, measurements of specific immune cell
597 types or cytokines in the bloodstream are unlikely to provide diagnostic value for autoimmunity in DS.
598 However, antigen-specific immune assays, such as T cell or B cell activation assays, may reveal the
599 specific timing of loss of tolerance and transition to clinical phenotypes. Future studies should also include
600 analysis of tissue-resident immune cells, which may identify sites of local autoimmune attack in DS.

601 Among the many strategies that could be used to attenuate IFN hyperactivity, JAK inhibitors are the
602 most well-studied and have the most approved indications[64]. Of the more than ten globally-approved JAK
603 inhibitors[64], we chose to employ in our clinical trial the JAK1/3 inhibitor tofacitinib, which is used to treat
604 diverse autoimmune/inflammatory conditions and which was approved in 2020 for treatment of
605 polyarticular course juvenile idiopathic arthritis (pcJIA) in children 2 years and older[64,65]. Notably, all four
606 IFNRs encoded on chr21 utilize JAK1 for signal transduction in combination with either JAK2 or TYK2,
607 making JAK1 inhibitors the most logical choice to dampen the effects of *IFNR* gene triplication. As part
608 of the clinical trial protocol, the approved interim analysis was designed to qualitatively evaluate
609 feasibility and initial safety data on the first 10 participants completing a 16-week course of tofacitinib
610 treatment. This analysis established that there were no AEs that required a change or cessation of
611 tofacitinib dosing and that this medicine is well tolerated in individuals with DS. The clear benefits
612 observed for diverse autoimmune skin conditions align with an increasing body of evidence supporting
613 the use of JAK inhibition for immunodermatological conditions, including their recent approval for
614 alopecia areata and atopic dermatitis in the general population[66,67]. At this sample size, the effects of
615 tofacitinib on HS are inconclusive. Although some participants and caregivers reported benefits in terms

616 of fewer flares of lesser severity, the MSS metric did not show a clear trend, which may reveal the need
617 for more frequent or different types of monitoring for HS, a condition that cycles periodically in severity.
618 Our results indicate that tofacitinib does not fully suppress the immune response in people with DS,
619 but rather attenuates IFN scores and cytokine scores to levels observed in the general population, which
620 is an important consideration given the likely requirement for long-term use of the drug in this population.
621 Furthermore, the effects of the drug are clearly gene-specific, highlighting the presence of inflammatory
622 processes that may not be attenuated with this inhibitor, which could be beneficial in terms of preserving
623 immune activity. Importantly, during treatment, both IFN scores and cytokine scores remain sensitive to
624 immune stimuli, as evidenced by participants who had received a vaccine or experienced an URI before a
625 blood draw (**Figure 6a**, **Figure 6 – figure supplement 1f**). Overall, it is encouraging that key
626 inflammatory markers decreased in a relatively short timeframe, likely offering systemic benefits beyond
627 skin pathology. Importantly, the fact that levels of IL-6 and TNF-α are reduced upon tofacitinib treatment
628 supports the use of JAK inhibitors over TNF-blockers or anti-IL-6 agents in this population. Although
629 TNF-α-blockers are recommended to be used first in the treatment of rheumatoid arthritis in the general
630 population[68], the value of this recommendation in people with DS remains to be defined. The clear
631 decrease in anti-TPO and anti-TG levels indicates that autoreactive B cell function requires elevated
632 JAK/STAT signaling, but whether this effect is cell-autonomous versus a consequence of a reduced
633 systemic inflammatory milieu will require further investigation. Defining the effect of tofacitinib on other
634 autoantibodies elevated in DS will also require a larger sample size and may be revealed in the full dataset
635 after completion of this trial.
636 Lastly, this ongoing clinical trial includes measurements of various dimensions of neurological
637 function not reported here. Although the absence of a placebo control arm may impede a clear
638 interpretation of any effect of JAK inhibition on cognitive function, preliminary results have prompted
639 the design and launch of a second trial (NCT05662228) aimed at defining the relative safety and efficacy
640 of tofacitinib, intravenous immunoglobulin (IVIG), and the benzodiazepine lorazepam for Down

641 syndrome Regression Disorder (DSRD), a condition characterized by sudden loss of neurological
642 function[69].
643 Altogether, these findings justify both a deeper investigation of all the deleterious effects of
644 autoimmunity and hyperinflammation in DS and the expanded testing of immunomodulatory strategies
645 for diverse aspects of DS pathophysiology, even perhaps from an early age.
646

647 **Materials and Methods.**

648 **Human Trisome Project (HTP) study.**

649 All aspects of this study were conducted in accordance with the Declaration of Helsinki under protocols
650 approved by the Colorado Multiple Institutional Review Board. Results and analyses presented herein are
651 part of a nested study within the Crnic Institute's Human Trisome Project (HTP, NCT02864108, see also
652 www.trisome.org) cohort study. All study participants, or their guardian/legally authorized representative,
653 provided written informed consent. The HTP study has generated multiple multi-omics datasets on
654 hundreds of research participants, some of which have been analyzed in previous studies, including whole
655 blood transcriptome data[42], white blood cell transcriptome data[19], plasma proteomics[42], plasma
656 metabolomics[19,42], and immune mapping via flow cytometry[16] and mass cytometry[42,48]. This paper reports
657 new analyses of select previous datasets (transcriptome, mass cytometry, MSD immune markers) within
658 the larger multi-omics dataset of the HTP study, as well as analyses of new datasets (e.g., anti-TPO, ANA,
659 autoantibodies), as described in detail below.

660 **Annotation of co-occurring conditions.**

661 Within the HTP, a clinical history for each participant is curated from both medical records and
662 participant/family reports. Both surveys are set up as REDCap[70] instruments that collect information as a
663 review of systems (e.g., cardiovascular, immunity, endocrine). Expert data curators complete the medical
664 record review and evaluate answers provided by self-advocates and caregivers. In cases of discordant
665 answers across the two instruments, medical records take precedence. De-identified demographic and
666 clinical metadata obtained is then linked to de-identified biospecimens used to generate the various -omics
667 (e.g., RNA sequencing) and targeted assay datasets (e.g., anti-TPO assays). For annotation of AITD,
668 several possible entries were considered as shown in **Figure 1 – figure supplement 1a**, including history
669 of hypothyroidism, hyperthyroidism, Hashimoto's disease, Grave's disease, anti-TPO or -TG antibodies,
670 and subclinical hypothyroidism. For annotation of immune skin conditions, atopic dermatitis and eczema

671 were combined and counted in a single group, as were hidradenitis suppurativa (HS), folliculitis, and
672 'boils'.

673 **Blood sample collection and processing.**

674 The biological datasets analyzed herein were derived from peripheral blood samples collected using
675 PAXgene RNA Tubes (Qiagen) and BD Vacutainer K2 EDTA tubes (BD). Whole blood from PAXgene
676 collection tubes was processed for RNA sequencing as described below. Two 0.5 mL aliquots of whole
677 blood were withdrawn from each EDTA tube and processed for mass cytometry as described below. The
678 remaining EDTA blood samples were centrifuged at 700 x g for 15 min to separate plasma, buffy coat
679 containing white blood cells (WBC), and red blood cells (RBCs). Samples were then aliquoted, flash
680 frozen and stored at -80°C until subsequent processing and analysis. Centrifugation and storage of samples
681 took place within 2 hours of collection.

682 **Measurements of autoantibodies.**

683 Anti-TPO status was determined from plasma samples using an electrochemiluminescence-based assay
684 [71], and carried out by the Autoantibody/HLA Core Facility of the Barbara Davis Center for Childhood
685 Diabetes at the University of Colorado Anschutz Medical Campus. Sample values were calculated as
686 (sample signal – negative control signal) / (positive control signal – negative control signal), with the
687 threshold (upper limit of normal) for TPO positivity based on the 95th percentile of healthy control
688 samples.

689 Anti-nuclear antigen (ANA) status was determined from plasma samples using a qualitative ELISA kit
690 (MyBioSource, cat. no. 702970) according to manufacturer instructions, with a sample OD_{450nm} / negative
691 control OD_{450nm} ratio ≥ 2.1 evaluated as positive and a ratio < 2.1 evaluated as negative.

692 Autoantigen profiling of EDTA plasma samples (50 µL each; T21, n = 120; D21, n = 60) was performed
693 by the Affinity Proteomics unit at SciLifeLab (KTH Royal Institute of Technology, Stockholm, Sweden)
694 using peptide arrays. Antigens were selected to cover potential associations to autoimmune diseases and
695 consisted of 380 peptide fragments covering ~270 unique proteins (1-5 fragments per protein). Fragments

696 were ~20-163 amino acids long (median 82). All antigens were expressed in E. coli with a hexahistidyl
697 and albumin binding protein tag (His6ABP). Using, COOH-NH2 chemistry, the analyzed antigens, in
698 addition to controls, were immobilized on color-coded magnetic beads (MagPlex, Luminex). Controls
699 consisted of His6ABP, buffer, rabbit anti-human IgG (loading control, Jackson ImmunoResearch), and
700 Epstein-Barr nuclear antigen 1 (EBNA1, Abcam). Research samples and technical controls (commercial
701 plasma; Seralab) were diluted (1:250) in assay buffer, which consisted of 3% BSA, 5% milk, 0.05%
702 Tween-20, and 160 μg/ml His6ABP tag in PBS. Diluted samples and controls were incubated for 1 hour
703 at room temperature then subsequently incubated with the antigen bead array for 2 hour. The reactions
704 were then fixed for 10 minutes using 0.02% paraformaldehyde, then incubated for 30 minutes with goat
705 Fab specific for human IgG Fc-γ tagged with the fluorescent marker R-phycoerythrin (Invitrogen). Median
706 fluorescence intensity (MFI) and number of beads for each reaction was analyzed using a FlexMap 3D
707 instrument (Luminex Corp.). Quality control was performed using MFI and bead count to exclude antigens
708 and samples not passing technical criteria including minimal bead counts and antigen coupling efficiency.
709 To adjust for sample specific backgrounds, MFI values were transformed per reaction median absolute
710 deviations (MADs) using the following calculation:

711 $$MADs_{sample} = (MFI - median_{sample(MFI)}) / MAD_{sample(MFI)}$$

712 Subsequent data analysis and handling was performed using R. For each antigen, positivity was defined
713 as >90th percentile MAD value for D21 samples only. Overrepresentation of positivity for each antigen
714 in the T21 versus D21 group was determined using Fisher's exact test, excluding antigens detected in <18
715 samples (<10% of total experiment). Correction for multiple testing was performed using the Benjamini-
716 Hochberg approach and significance defined as q<0.1 (10% FDR). Similarly, within the T21 group,
717 Fisher's exact test was used to test for overrepresentation of antigen positivity in cases versus controls for
718 co-occurring conditions, with only those with at least 5 cases considered in the analysis.

719 **Immune profiling via mass cytometry.**

720 Generation of the mass cytometry dataset was described previously[42], but a full description is included
721 here for reference. Two 0.5 mL aliquots of EDTA whole blood samples underwent RBC lysis and white
722 blood cell fixation using TFP FixPerm Buffer (Transcription Factor Phospho Buffer Set, BD Biosciences).
723 WBCs were then washed in 1x in PBS (Rockland), resuspended in Cell Staining Buffer (Fluidigm) and
724 stored at −80°C. For antibody staining, samples were thawed at room temperature, washed in Cell Staining
725 Buffer, barcoded using a Cell-ID 20-Plex Pd Barcoding Kit (Fluidigm), and combined per batch. Each
726 batch was able to accommodate 19 samples with a common reference sample. Antibodies were either
727 purchased pre-conjugated to metal isotopes or conjugation was performed in-house using a Maxpar
728 Antibody Labeling Kit (Fluidigm). See **Supplementary file 7** for antibodies. Working dilutions for
729 antibody staining were titrated and validated using the common reference sample and comparison to
730 relative frequencies obtained by independent flow cytometry analysis. Surface marker staining was carried
731 out for 30 min at 4°C in Cell Staining Buffer with added Fc Receptor Binding Inhibitor
732 (eBioscience/ThermoFisher Scientific). Staining was followed by a wash in Cell Staining Buffer. Next,
733 cells were permeabilized in Buffer III (Transcription Factor Phospho Buffer Set, BD Pharmingen) for 20
734 min at 4°C followed by washing with perm/wash buffer (Transcription Factor Phospho Buffer Set, BD
735 Pharmingen). Intracellular transcription factor and phospho-epitope staining was carried out for 1 hour at
736 4°C in perm/wash buffer (Transcription Factor Phospho Buffer Set, BD Pharmingen), followed by a wash
737 with Cell Staining Buffer. Cell-ID Intercalator-Ir (Fluidigm) was used to label barcoded and stained cells.
738 Labeled cells were analyzed on a Helios instrument (Fluidigm). Mass cytometry data were exported as
739 v3.0 FCS files for pre-processing and analysis.

740 *Analysis of mass cytometry data.*

741 *Pre-processing.* Bead-based normalization via polystyrene beads embedded with lanthanides, both within
742 and between batches, followed by bead removal was carried out as previously described using the Matlab-
743 based Normalizer tool[72]. Batched FCS files were demultiplexed using the Matlab-based Single Cell
744 Debarcoder tool[73]. Reference-based normalization of individual samples across batches against the

745 common reference sample was then carried out using the R script *BatchAdjust()*. For the analyses
746 described in this manuscript, CellEngine (CellCarta) was used to gate and export per-sample FCS files at
747 four levels: Firstly, CD3+CD19+ doublets were excluded and remaining cells exported as 'Live' cells;
748 Live cells were then gated for hematopoietic lineage (CD45-positive) non-granulocytic (CD66-low) cells
749 and exported as CD45+CD66low. Lastly, CD45+CD66low cells were gated on CD3-positivity and CD19-
750 positivity and exported as T- and B-cells, respectively. Per-sample FCS files were then subsampled to a
751 maximum of 50,000 events per file for subsequent analysis.
752 *Unsupervised clustering.* For each of the four levels (live, non-granulocytes, T cells, and B cells), all 388
753 per-sample FCS files were imported into R as a flowSet object using the *read.flowSet()* function from the
754 flowCore R package[74]. Next a SingleCellExperiment object was constructed from the flowSet object using
755 the *prepData()* function from the CATALYST package[75]. Arcsinh transformation was applied to marker
756 expression data with cofactor values ranging from ~0.2 to ~15 to give optimal separation of positive and
757 negative populations for each marker, using the *estParamFlowVS()* function from the flowVS R package[76]
758 and based on visual inspection of marker histograms (see **Supplementary file 7)**. Quality control and
759 diagnostic plots were examined with the help of functions from CATALYST and the
760 tidySingleCellExperiment R package. Unsupervised clustering using the FlowSOM algorithm[43] was
761 carried out using the *cluster()* function from CATALYST, with grid size set to 10 x 10 to give 100 initial
762 clusters and a maxK value of 40 was explored for subsequent meta-clustering using the
763 ConsensusClusterPlus algorithm. Examination of delta area and minimal spanning tree plots indicated that
764 30-40 meta clusters gave a reasonable compromise between gains in cluster stability and number of
765 clusters for each level. Each clustering level was re-run with multiple random seed values to ensure
766 consistent results.
767 *Visualization using t-distributed stochastic neighbor imbedding (tSNE).* Dimensionality reduction to two
768 dimensions was carried out using the *runDR()* function from the CATALYST package, with 500 cells per
769 sample, and using several random seed values to ensure consistent results. Multiple values of the

770 perplexity parameter were tested, with a setting of 440, using the formula Perplexity=N^(1/2) as suggested
771 at https://towardsdatascience.com/how-to-tune-hyperparameters-of-tsne-7c0596a18868, providing a
772 visualization with good agreement with the clusters defined by FlowSOM.
773 *Cell type classification.* To aid in assignment of clusters to specific lineages and cell types, the MEM
774 package (marker enrichment modeling) was used to call positive and negative markers for each cell cluster
775 based on marker expression distributions across clusters. Manual review and comparison to marker
776 expression histograms, as well as minimal spanning tree plots and tSNE plots colored by marker
777 expression, allowed for high-confidence assignment of most clusters to specific cell types. Clusters that
778 were insufficiently distinguishable were merged into their nearest cluster based on the minimal spanning
779 tree. Relative frequencies for each cell type / cluster were calculated for each sample as a percentage of
780 total live cells and as a percentage of cells used for each level of clustering: total CD45+CD66low cells,
781 total T cells, or total B cells.
782 *Beta regression analysis.* To identify cell clusters for which relative frequencies are associated with either
783 trisomy 21 status or with various clinical subgroups (e.g. ANA+) among individuals with trisomy 21, beta
784 regression analysis was carried out using the betareg R package, with each model using cell type cluster
785 proportions (relative frequency) as the outcome/dependent variable and either T21 status or clinical
786 subgroups as independent/predictor variables, along with adjustment for age and sex, and a logit link
787 function. Extreme outliers were classified per-karyotype and per-cluster as measurements more than three
788 times the interquartile range below or above the first and third quartiles, respectively (below Q1 - 3*IQR
789 or above Q3 + 3*IQR) and excluded from beta regression analysis. Correction for multiple comparisons
790 was performed using the Benjamini-Hochberg (FDR) approach. Effect sizes (as fold-change in T21 vs.
791 euploid controls or among T21 subgroups) for each cell type cluster were obtained by exponentiation of
792 beta regression model coefficients. Fold-changes were visualized by overlaying on tSNE plots using
793 ggplot2. For visualization of individual clusters, data points were adjusted for age and sex, using the

794 *adjust()* function from the datawizard R package, and visualized as sina plots (separated by T21 status or
795 clinical subgroup).

796 **Measurement of immune markers and calculation of cytokine scores.**

797 Briefly, from each EDTA plasma sample, two replicates of 12-25 μL were analyzed using the Meso Scale
798 Discovery (MSD) multiplex immunoassay platform V-PLEX Human Biomarker 54-Plex Kit (HTP
799 cohort) or U-PLEX Human Biomarker Group 1 71-Plex and V-PLEX Human Vascular Injury Panel 2
800 Kits (clinical trial cohort) on a MESO QuickPlex SQ 120 instrument. Assays were carried out as per
801 manufacturer instructions. Concentration values were calculated against a standard curve with provided
802 calibrators. MSD data are reported as concentration values in picograms per milliliter of plasma.

803 *Analysis of immune marker data.* Plasma concentration values (pg/mL) for each of the cytokines and
804 related immune factors measured across multiple MSD assay plates was imported to R, combined, and
805 analytes with >10% of values outside of detection or fit curve range flagged. For each analyte, missing
806 values were replaced with either the minimum (if below fit curve range) or maximum (if above fit curve
807 range) calculated concentration per plate/batch and means of duplicate wells used for subsequent analysis.
808 For the HTP study analysis, extreme outliers were classified per-karyotype and per-analyte as
809 measurements more than three times the interquartile range below or above the first and third quartiles,
810 respectively, and excluded from further analysis. Differential abundance analysis for inflammatory
811 markers measured by MSD was performed using mixed effects linear regression as implemented in the
812 *lmer()* function from the lmerTest R package (v3.1-2) with log2-transformed concentration as the
813 outcome/dependent variable, T21 status or clinical subgroup (e.g., ANA+) as the predictor/independent
814 variable, age and sex as fixed covariates, and sample source as a random effect. Multiple hypothesis
815 correction was performed with the Benjamini-Hochberg method using a false discovery rate (FDR)
816 threshold of 10% ($q < 0.1$). Prior to visualization or correlation analysis, MSD data were adjusted for age,
817 sex, and sample source using the *removeBatchEffect()* function from the limma package (v3.44.3).

818 *Calculation of cytokine scores.* For comparison of clinical trial samples across time points, cytokine scores
819 were calculated as the sum of the Z-scores for TNF-α, IL-6, CRP and IP-10. For comparison of clinical
820 trial samples to the HTP cohort, Z-scores were first calculated from age-, sex, and batch-adjusted values
821 for each sample, based on the mean and standard deviation of the HTP euploid control samples.

822 **Whole blood transcriptome analysis and calculation of IFN scores.**

823 Strand-specific sequencing libraries were prepared from globin-depleted, polyA-enriched whole blood
824 RNA and sequenced on the Illumina NovaSeq platform (2x 150 bases). Data quality was assessed using
825 FASTQC (v0.11.5) and FastQ Screen (v0.11.0). Trimming and filtering of low-quality reads was
826 performed using bbduk from BBTools (v37.99) and fastq-mcf from ea-utils (v1.05). Alignment to the
827 human reference genome (GRCh38) was carried out using HISAT2 (v2.1.0) in paired, spliced-alignment
828 mode against a GRCh38 index and Gencode v33 basic annotation GTF, and alignments were sorted and
829 filtered for mapping quality (MAPQ > 10) using Samtools (v1.5). Gene-level count data were quantified
830 using HTSeq-count (v0.6.1) with the following options (--stranded=reverse –minaqual=10 –type=exon --
831 mode=intersection-nonempty) using a Gencode v33 GTF annotation file. Differential gene expression in
832 T21 versus D21 was evaluated using DESeq2 (version 1.28.1)[77], with $q < 0.1$ (10% FDR) as the threshold
833 for differential expression.

834 *DS IFN scores.* RNA-seq-based 'Down syndrome interferon scores' (DS IFN scores) were calculated as
835 follows: for comparison of clinical trial samples across time points, DS IFN scores were calculated as the
836 sum of Z-scores across 16 interferon-stimulated genes (ISGs) genes with significant mean fold-change of
837 at least 1.5 in the HTP T21 group vs. the euploid control group, excluding *IFNAR2*, *MX1*, and *MX2* which
838 are encoded on chromosome 21. For comparison of clinical trial samples to the HTP cohort, gene-wise Z-
839 scores were first calculated from age-, sex, and sequencing batch-adjusted FPKM values for each sample,
840 based on the mean and standard deviation of the HTP euploid control samples.

841 *Gene set enrichment analysis (GSEA).* GSEA[78] was carried out in R using the fgsea package (v1.14.0),
842 using Hallmark gene sets, log_2-transformed fold-change values as the ranking metric.

843 **Clinical trial design and oversight.**

844 All aspects of this study were conducted in accordance with the Declaration of Helsinki. All study
845 activities were approved by the Colorado Multiple Institutional Review Board (COMIRB, protocol # 19-
846 1362, NCT04246372) with an independent Data and Safety Monitoring Board (DSMB) appointed by the
847 National Institute of Arthritis and Musculoskeletal and Skin Diseases (NIAMS). Written consent was
848 obtained from all participants, or their legally authorized representative if the participant was unable to
849 provide consent, in which case participant assent was obtained. The Clinical Trial Protocol is provided in
850 the **Supplementary file 8**. We report here interim results of a single-site, open-label phase 2 clinical trial
851 enrolling individuals with DS between the ages of 12 and 50 years old with moderate-to-severe alopecia
852 areata, hidradenitis suppurativa, psoriasis, atopic dermatitis, or vitiligo. Qualifying disease scores are
853 shown in **Supplementary file 3**. After screening, qualifying participants are prescribed 5 mg tofacitinib
854 twice daily for 16 weeks, with an optional extension arm to week 40. During the main 16-week trial,
855 participants attend five safety monitoring visits after enrollment at the Baseline visit.

856 **Trial Population.**

857 The recruitment goal for this trial is 40 participants completing 16 weeks of tofacitinib treatment, with a
858 qualitative interim analysis triggered when 10 participants completed the main 16-week trial. Of the 10
859 participants included in the interim analysis, 4 are female, 100% identify as White/Caucasian, 3 identify
860 as Hispanic or Latino, and mean age at enrollment was 23.1 years old (range 15-38.1 years old)
861 (**Supplementary file 3**). Baseline qualifying conditions of the 10 participants were alopecia areata: n=6
862 (46.1%), hidradenitis suppurativa: n=3 (30.8%), or psoriasis: n=1 (7.7%). Two participants also had atopic
863 dermatitis, and two others had vitiligo, albeit below the severity required to be the qualifying condition.

864 **Outcome Measures.**

865 *Primary endpoints.* The two primary outcome measures for this trial are safety and reduction in IFN
866 transcriptional scores derived from peripheral whole blood. Based on the safety profile for tofacitinib in
867 the general population[68], the safety primary endpoint was defined as no more than two serious adverse
868 events (SAEs) definitely attributable to tofacitinib over the course of 16 weeks for 40 participants. Adverse
869 events were classified based using Common Terminology Criteria for Adverse Events 5.0 (CTCAE 5.0).
870 IFN scores are commonly used to monitor disease severity and response to treatment in IFN-driven
871 pathologies[79,80] and their calculation form RNAseq data is described above.
872 *Secondary endpoints.* The secondary outcome measures for this trial include improvements in skin health
873 as defined by a global assessment, the Investigator Global Assessment (IGA), as well as the disease-
874 specific assessments. Overall skin pathology, accounting for all present skin conditions regardless of
875 severity, was assessed using a modified IGA which scores on a five-point scale for each skin condition
876 (six points for HS) with a range of 0-21. Another secondary endpoint assessing global skin health is a
877 change in the Dermatological Quality of Life Index (DLQI), used to assess participant-reported impact of
878 skin conditions on self-image, relationships, and daily activities. Possible total scores range from 0-30,
879 with higher scores indicating a more impaired quality of life. Condition-specific assessments used are
880 Severity of Alopecia Tool (SALT) for AA affecting at least 25% of the scalp (qualifying score is ≥ 25);
881 Hidradenitis Suppurativa-Physicians Global Assessment (HS-PGA) to define eligibility (qualifying score
882 ≥3) and Modified Sartorius Scale (MSS) to monitor changes throughout the study for HS; Psoriasis Area
883 and Severity Index (PASI, qualifying score is ≥10) for psoriasis; Vitiligo Extent Tensity Index (VETI,
884 qualifying score is ≥2), for moderate-to-severe vitiligo; and Eczema Area and Severity Index (EASI,
885 qualifying EASI score ≥16) for moderate-to-severe atopic dermatitis. The last secondary endpoint is
886 reduction in a cytokine score coalescing information on four inflammatory markers elevated in DS: Tumor
887 Necrosis Factor Alpha (TNF-α), interleukin 6 (IL-6), C-reactive protein (CRP), and IFN-inducible protein
888 10 (IP10, CXCL10)[18]. Measurement of these proteins and calculation of the cytokine score is described
889 above.

890 *Tertiary endpoints.* This clinical trial includes multiple exploratory tertiary endpoints (see full protocol in
891 **Supplementary file 8**), including reduction in autoantibodies related to AITD (anti-TPO, anti-TG, and
892 anti-TSHr) and celiac disease (anti-tTG, anti-DGP) . In the clinical trial, these autoantibodies were
893 assessed using established clinical assays.

894 **Statistical Analysis.**

895 The Statistical Analysis Plan (SAP) approved by the appointed DSMB is included with the Clinical Trial
896 Protocol in the **Supplementary file 8**. This report includes analysis of the time points used to assess
897 endpoints (baseline and 16 weeks), as well research-only time points at 2 and 8 weeks of treatment. Given
898 the qualitative nature of this interim analysis, statistical analysis is not completed for changes observed
899 between baseline and the 16-week endpoint. Data may be displayed as $\log_2$ transformed for clarity in
900 viewing the graphs.

901

902 **Data Availability Statement:**

903 A collection with datasets used in this study is available in Synapse
904 (https://doi.org/10.7303/syn53185135), with the individual datasets also accessible as detailed below.
905 Demographic and health history data for research participants in the HTP study are available on both the
906 Synapse data sharing platform (https://doi.org/10.7303/syn31488784) and through the INCLUDE Data
907 Hub (https://portal.includedcc.org/). Mass cytometry data for 380+ HTP research participants are
908 available both in Synapse (https://doi.org/10.7303/syn53185253) and FlowRepository, Study ID FR-
909 FCM-Z5GE,
910 https://flowrepository.org/id/RvFrQaBqhe8TGyko1OMdQKtR7HN8nulAnHW0PJkm1CEyyo8fnJg2rHr
911 WvNrhE8xu. Targeted plasma proteomics for inflammatory markers using Meso Scale Discovery (MSD)
912 assays for 470+ HTP research participants can be accessed through Synapse
913 (https://doi.org/10.7303/syn31475487) and the INCLUDE Data Hub. Whole blood transcriptome data for
914 400 HTP research participants can be accessed through Synapse (https://doi.org/10.7303/syn31488780),

915 the INCLUDE Data Hub, and NCBI Gene Expression Omnibus (GSE190125). Whole blood
916 transcriptome data for 10 clinical trial participants at baseline and after 2, 8, and 16 weeks of tofacitinib
917 treatment can be accessed through Synapse (https://doi.org/10.7303/syn53185250), and NCBI Gene
918 Expression Omnibus (GSE PENDING). Targeted plasma proteomics for inflammatory markers using
919 Meso Scale Discovery (MSD) assays for 10 clinical trial participants can be accessed through Synapse
920 (https://doi.org/10.7303/syn53185252).

921

922 **Code Availability Statement:** No custom code or algorithms were developed during the course of this
923 study. R analysis scripts will be made available upon request.

924

925 **References.**

926 1 Lejeune, J., Turpin, R. & Gautier, M. [Mongolism; a chromosomal disease (trisomy)]. *Bull Acad*
927 *Natl Med* **143**, 256-265 (1959).

928 2 Antonarakis, S. E. *et al.* Down syndrome. *Nature reviews. Disease primers* **6**, 9 (2020).
929 https://doi.org:10.1038/s41572-019-0143-7

930 3 Chicoine, B. *et al.* Prevalence of Common Disease Conditions in a Large Cohort of Individuals
931 With Down Syndrome in the United States. *J Patient Cent Res Rev* **8**, 86-97 (2021).
932 https://doi.org:10.17294/2330-0698.1824

933 4 Amr, N. H. Thyroid Disorders in Subjects with Down Syndrome: An Update. *Acta Biomed* **89**,
934 132-139 (2018). https://doi.org:10.23750/abm.v89i1.7120

935 5 Pierce, M. J., LaFranchi, S. H. & Pinter, J. D. Characterization of Thyroid Abnormalities in a
936 Large Cohort of Children with Down Syndrome. *Hormone research in paediatrics* **87**, 170-178
937 (2017). https://doi.org:10.1159/000457952

938 6 Iughetti, L. *et al.* Ten-year longitudinal study of thyroid function in children with Down's
939 syndrome. *Hormone research in paediatrics* **82**, 113-121 (2014).
940 https://doi.org:10.1159/000362450

941 7 Book, L. *et al.* Prevalence and clinical characteristics of celiac disease in Downs syndrome in a
942 US study. *American journal of medical genetics* **98**, 70-74 (2001).

943 8 Zachor, D. A., Mroczek-Musulman, E. & Brown, P. Prevalence of celiac disease in Down
944 syndrome in the United States. *Journal of pediatric gastroenterology and nutrition* **31**, 275-279
945 (2000).

946 9 Sureshbabu, R. *et al.* Phenotypic and dermatological manifestations in Down Syndrome.
947 *Dermatology online journal* **17**, 3 (2011).

948 10 Madan, V., Williams, J. & Lear, J. T. Dermatological manifestations of Down's syndrome.
949 *Clinical and experimental dermatology* **31**, 623-629 (2006). https://doi.org:10.1111/j.1365-
950 2230.2006.02164.x
951 11 Lam, M., Lai, C., Almuhanna, N. & Alhusayen, R. Hidradenitis suppurativa and Down
952 syndrome: A systematic review and meta-analysis. *Pediatric dermatology* **37**, 1044-1050 (2020).
953 https://doi.org:10.1111/pde.14326
954 12 Araya, P. *et al.* IGF1 deficiency integrates stunted growth and neurodegeneration in Down
955 syndrome. *Cell reports* **41**, 111883 (2022). https://doi.org:10.1016/j.celrep.2022.111883
956 13 Flores-Aguilar, L. *et al.* Evolution of neuroinflammation across the lifespan of individuals with
957 Down syndrome. *Brain* **143**, 3653-3671 (2020). https://doi.org:10.1093/brain/awaa326
958 14 Wilcock, D. M. & Griffin, W. S. T. Down's syndrome, neuroinflammation, and Alzheimer
959 neuropathogenesis. *Journal of neuroinflammation* **10**, 864 (2013). https://doi.org:10.1186/1742-
960 2094-10-84
961 15 Waugh, K. A. *et al.* Mass Cytometry Reveals Global Immune Remodeling with Multi-lineage
962 Hypersensitivity to Type I Interferon in Down Syndrome. *Cell reports* **29**, 1893-1908 e1894
963 (2019). https://doi.org:10.1016/j.celrep.2019.10.038
964 16 Araya, P. *et al.* Trisomy 21 dysregulates T cell lineages toward an autoimmunity-prone state
965 associated with interferon hyperactivity. *Proc Natl Acad Sci U S A* **116**, 24231-24241 (2019).
966 https://doi.org:10.1073/pnas.1908129116
967 17 Sullivan, K. D. *et al.* Trisomy 21 consistently activates the interferon response. *Elife* **5** (2016).
968 https://doi.org:10.7554/eLife.16220
969 18 Sullivan, K. D. *et al.* Trisomy 21 causes changes in the circulating proteome indicative of
970 chronic autoinflammation. *Scientific reports* **7**, 14818 (2017). https://doi.org:10.1038/s41598-
971 017-13858-3

19 Powers, R. K. *et al.* Trisomy 21 activates the kynurenine pathway via increased dosage of interferon receptors. *Nat Commun* **10**, 4766 (2019). https://doi.org:10.1038/s41467-019-12739-9

20 Secombes, C. J. & Zou, J. Evolution of Interferons and Interferon Receptors. *Front Immunol* **8**, 209 (2017). https://doi.org:10.3389/fimmu.2017.00209

21 Waugh, K. A., Minter, R., Baxter, J., Chi, C., Tuttle, K.D., Eduthan, N.P., Galbraith, M.D., Kinning, K.T., Andrysik, Z., Araya, P., Dougherty, H., Dunn, L.N., Ludwig, M., Schade, K.A., Tracy, D., Smith, K.P., Granrath, R.E., Busquet, N., Khanal, S., Anderson, R.D., Cox, L.L., BEnriquez Estrada, B., Rachubinski, A.L., Lyford, H.R., Britton, E.C., Orlicky, D.J., Matsuda, J.L., Song, K., Cox, T.C., Sullivan, K.D., and Espinosa, J.M. Interferon receptor gene dosage determines diverse hallmarks of Down syndrome. *BioRxiv* (2022). https://doi.org:https://doi.org/10.1101/2022.02.03.478982

22 Tuttle, K. D. *et al.* JAK1 Inhibition Blocks Lethal Immune Hypersensitivity in a Mouse Model of Down Syndrome. *Cell reports* **33**, 108407 (2020). https://doi.org:10.1016/j.celrep.2020.108407

23 Galbraith, M. D., Rachubinski, A.L., Smith, K.P., Araya, P., Waugh, K.A., Enriquez-Estrada, B., Worek, K., Granrath, R.E., Kinning, K.T., Eduthan, N.P., Ludwig, M.P. Hsieh, E.W.Y., Sullivan, K.D., Espinosa, J.M. Multidimensional definition of the interferonopathy of Down syndrome and its response to JAK inhibition. *Science Advances* **9** (2023).

24 Chi, C., Knight, W.E., Riching, A.S., Zhang, Z., Tatavosian, R., Zhuang, Y., Moldovan, R., Rachubinski, A.L., Gao, D., Xu H., Espinosa, J.M., Song, K. . Interferon hyperactivity impairs cardiogenesis in Down syndrome via downregulation of canonical Wnt signaling. *iScience* **26, 107012** (2023). https://doi.org:https://doi.org/10.1016/j.isci. 2023.107012

25 Lambert, K. *et al.* Deep immune phenotyping reveals similarities between aging, Down syndrome, and autoimmunity. *Science translational medicine* **14**, eabi4888 (2022). https://doi.org:10.1126/scitranslmed.abi4888

997 26 Khor, B. & Buckner, J. H. Down syndrome: insights into autoimmune mechanisms. *Nature*
998 *reviews. Rheumatology*, 1-2 (2023). https://doi.org:10.1038/s41584-023-00970-0
999 27 Gensous, N., Bacalini, M. G., Franceschi, C. & Garagnani, P. Down syndrome, accelerated aging
000 and immunosenescence. *Seminars in immunopathology* (2020). https://doi.org:10.1007/s00281-
001 020-00804-1
002 28 Malle, L. *et al.* Autoimmunity in Down's syndrome via cytokines, CD4 T cells and CD11c(+) B
003 cells. *Nature* **615**, 305-314 (2023). https://doi.org:10.1038/s41586-023-05736-y
004 29 Aversa, T. *et al.* Epidemiological and clinical aspects of autoimmune thyroid diseases in children
005 with Down's syndrome. *Ital J Pediatr* **44**, 39 (2018). https://doi.org:10.1186/s13052-018-0478-9
006 30 Liu, E. *et al.* Routine Screening for Celiac Disease in Children With Down Syndrome Improves
007 Case Finding. *Journal of pediatric gastroenterology and nutrition* **71**, 252-256 (2020).
008 https://doi.org:10.1097/mpg.0000000000002742
009 31 Johnson, M. B. *et al.* Trisomy 21 Is a Cause of Permanent Neonatal Diabetes That Is
010 Autoimmune but Not HLA Associated. *Diabetes* **68**, 1528-1535 (2019).
011 https://doi.org:10.2337/db19-0045
012 32 Aitken, R. J. *et al.* Early-onset, coexisting autoimmunity and decreased HLA-mediated
013 susceptibility are the characteristics of diabetes in Down syndrome. *Diabetes Care* **36**, 1181-
014 1185 (2013). https://doi.org:10.2337/dc12-1712
015 33 Singh, P. *et al.* Global Prevalence of Celiac Disease: Systematic Review and Meta-analysis. *Clin*
016 *Gastroenterol Hepatol* **16**, 823-836 e822 (2018). https://doi.org:10.1016/j.cgh.2017.06.037
017 34 Markle, J. G. *et al.* Sex differences in the gut microbiome drive hormone-dependent regulation of
018 autoimmunity. *Science* **339**, 1084-1088 (2013). https://doi.org:10.1126/science.1233521
019 35 Molano-Gonzalez, N. *et al.* Cluster analysis of autoimmune rheumatic diseases based on
020 autoantibodies. New insights for polyautoimmunity. *Journal of autoimmunity* **98**, 24-32 (2019).
021 https://doi.org:10.1016/j.jaut.2018.11.002

022 36 Elling, C. L. *et al.* Otitis Media in Children with Down Syndrome Is Associated with Shifts in
023 the Nasopharyngeal and Middle Ear Microbiotas. *Genet Test Mol Biomarkers* **27**, 221-228
024 (2023). https://doi.org:10.1089/gtmb.2023.0132
025 37 Ghazanfari, N., Morsch, M., Reddel, S. W., Liang, S. X. & Phillips, W. D. Muscle-specific
026 kinase (MuSK) autoantibodies suppress the MuSK pathway and ACh receptor retention at the
027 mouse neuromuscular junction. *J Physiol* **592**, 2881-2897 (2014).
028 https://doi.org:10.1113/jphysiol.2013.270207
029 38 Poulter, J. A. *et al.* Novel somatic mutations in UBA1 as a cause of VEXAS syndrome. *Blood*
030 **137**, 3676-3681 (2021). https://doi.org:10.1182/blood.2020010286
031 39 Lin, S. J. *et al.* Biallelic variants in WARS1 cause a highly variable neurodevelopmental
032 syndrome and implicate a critical exon for normal auditory function. *Hum Mutat* **43**, 1472-1489
033 (2022). https://doi.org:10.1002/humu.24435
034 40 Allenbach, Y., Benveniste, O., Stenzel, W. & Boyer, O. Immune-mediated necrotizing
035 myopathy: clinical features and pathogenesis. *Nature reviews. Rheumatology* **16**, 689-701
036 (2020). https://doi.org:10.1038/s41584-020-00515-9
037 41 Amagai, M., Nishikawa, T., Nousari, H. C., Anhalt, G. J. & Hashimoto, T. Antibodies against
038 desmoglein 3 (pemphigus vulgaris antigen) are present in sera from patients with paraneoplastic
039 pemphigus and cause acantholysis in vivo in neonatal mice. *The Journal of clinical investigation*
040 **102**, 775-782 (1998). https://doi.org:10.1172/JCI3647
041 42 Galbraith, M. D. *et al.* Multidimensional definition of the interferonopathy of Down syndrome
042 and its response to JAK inhibition. *Science Advances* **9**, eadg6218 (2023).
043 https://doi.org:doi:10.1126/sciadv.adg6218
044 43 Van Gassen, S. *et al.* FlowSOM: Using self-organizing maps for visualization and interpretation
045 of cytometry data. *Cytometry A* **87**, 636-645 (2015). https://doi.org:10.1002/cyto.a.22625

046 44 Amini, A., Pang, D., Hackstein, C. P. & Klenerman, P. MAIT Cells in Barrier Tissues: Lessons
047 from Immediate Neighbors. *Front Immunol* **11**, 584521 (2020).
048 https://doi.org:10.3389/fimmu.2020.584521
049 45 Zhang, Y. *et al.* Aberrations in circulating inflammatory cytokine levels in patients with Down
050 syndrome: a meta-analysis. *Oncotarget* **8**, 84489-84496 (2017).
051 https://doi.org:10.18632/oncotarget.21060
052 46 Kusters, M. A., Gemen, E. F., Verstegen, R. H., Wever, P. C. & E, D. E. V. Both normal
053 memory counts and decreased naive cells favor intrinsic defect over early senescence of Down
054 syndrome T lymphocytes. *Pediatr Res* **67**, 557-562 (2010).
055 https://doi.org:10.1203/PDR.0b013e3181d4eca3
056 47 Trotta, M. B. *et al.* Inflammatory and Immunological parameters in adults with Down syndrome.
057 *Immun Ageing* **8**, 4 (2011). https://doi.org:10.1186/1742-4933-8-4
058 48 Waugh, K. A. *et al.* Triplication of the interferon receptor locus contributes to hallmarks of
059 Down syndrome in a mouse model. *Nature genetics* (2023). https://doi.org:10.1038/s41588-023-
060 01399-7
061 49 Rachubinski, A. L. *et al.* Janus kinase inhibition in Down syndrome: 2 cases of therapeutic
062 benefit for alopecia areata. *JAAD Case Rep* **5**, 365-367 (2019).
063 https://doi.org:10.1016/j.jdcr.2019.02.007
064 50 Pham, A. T. *et al.* JAK inhibition for treatment of psoriatic arthritis in Down syndrome.
065 *Rheumatology* (2021). https://doi.org:10.1093/rheumatology/keab203
066 51 Guild, A., Fritch, J., Patel, S., Reinhardt, A. & Acquazzino, M. Hemophagocytic
067 lymphohistocytosis in trisomy 21: successful treatment with interferon inhibition. *Pediatr*
068 *Rheumatol Online J* **20**, 104 (2022). https://doi.org:10.1186/s12969-022-00764-w

069 52 Cohen, S. B. *et al.* Long-term safety of tofacitinib for the treatment of rheumatoid arthritis up to
070 8.5 years: integrated analysis of data from the global clinical trials. *Ann Rheum Dis* **76**, 1253-
071 1262 (2017). https://doi.org:10.1136/annrheumdis-2016-210457
072 53 Honda, K., Takaoka, A. & Taniguchi, T. Type I interferon [corrected] gene induction by the
073 interferon regulatory factor family of transcription factors. *Immunity* **25**, 349-360 (2006).
074 https://doi.org:10.1016/j.immuni.2006.08.009
075 54 Schwartz, D. M. *et al.* JAK inhibition as a therapeutic strategy for immune and inflammatory
076 diseases. *Nature reviews. Drug discovery* **17**, 78 (2017). https://doi.org:10.1038/nrd.2017.267
077 55 Schwartz, D. M., Bonelli, M., Gadina, M. & O'Shea, J. J. Type I/II cytokines, JAKs, and new
078 strategies for treating autoimmune diseases. *Nature reviews. Rheumatology* **12**, 25-36 (2016).
079 https://doi.org:10.1038/nrrheum.2015.167
080 56 Maroun, L. E., Heffernan, T. N. & Hallam, D. M. Partial IFN-alpha/beta and IFN-gamma
081 receptor knockout trisomy 16 mouse fetuses show improved growth and cultured neuron
082 viability. *Journal of interferon & cytokine research : the official journal of the International*
083 *Society for Interferon and Cytokine Research* **20**, 197-203 (2000).
084 https://doi.org:10.1089/107999000312612
085 57 Bhattacharya, S., Cherry, C., Deutsch, G., Birth Defects Research Laboratory (BDRL), Glass,
086 I.A., Mariani, T.J., Al Alam, D., Danopoulos, S. A Trisomy 21 Lung Cell Atlas. *bioRxiv* **doi:**
087 **https://doi.org/10.1101/2023.03.30.534839** (2023). https://doi.org:doi:
088 https://doi.org/10.1101/2023.03.30.534839
089 58 Aziz, N. M. *et al.* Lifespan analysis of brain development, gene expression and behavioral
090 phenotypes in the Ts1Cje, Ts65Dn and Dp(16)1/Yey mouse models of Down syndrome. *Dis*
091 *Model Mech* **11** (2018). https://doi.org:10.1242/dmm.031013

092 59 Rodero, M. P. & Crow, Y. J. Type I interferon-mediated monogenic autoinflammation: The type
093 I interferonopathies, a conceptual overview. *The Journal of experimental medicine* **213**, 2527-
094 2538 (2016). https://doi.org:10.1084/jem.20161596
095 60 Breslin, N. K., Varadarajan, V. V., Sobel, E. S. & Haberman, R. S. Autoimmune inner ear
096 disease: A systematic review of management. *Laryngoscope Investig Otolaryngol* **5**, 1217-1226
097 (2020). https://doi.org:10.1002/lio2.508
098 61 Kocyigit, M. *et al.* Association Between Endocrine Diseases and Serous Otitis Media in
099 Children. *J Clin Res Pediatr Endocrinol* **9**, 48-51 (2017). https://doi.org:10.4274/jcrpe.3585
100 62 Ercolini, A. M. & Miller, S. D. The role of infections in autoimmune disease. *Clin Exp Immunol*
101 **155**, 1-15 (2009). https://doi.org:10.1111/j.1365-2249.2008.03834.x
102 63 Dresser, L., Wlodarski, R., Rezania, K. & Soliven, B. Myasthenia Gravis: Epidemiology,
103 Pathophysiology and Clinical Manifestations. *J Clin Med* **10** (2021).
104 https://doi.org:10.3390/jcm10112235
105 64 Shawky, A. M., Almalki, F. A., Abdalla, A. N., Abdelazeem, A. H. & Gouda, A. M. A
106 Comprehensive Overview of Globally Approved JAK Inhibitors. *Pharmaceutics* **14** (2022).
107 https://doi.org:10.3390/pharmaceutics14051001
108 65 Ruperto, N. *et al.* Tofacitinib in juvenile idiopathic arthritis: a double-blind, placebo-controlled,
109 withdrawal phase 3 randomised trial. *Lancet* **398**, 1984-1996 (2021).
110 https://doi.org:10.1016/S0140-6736(21)01255-1
111 66 King, B. A. & Craiglow, B. G. Janus kinase inhibitors for alopecia areata. *Journal of the*
112 *American Academy of Dermatology* **89**, S29-S32 (2023).
113 https://doi.org:10.1016/j.jaad.2023.05.049
114 67 Tampa, M., Mitran, C. I., Mitran, M. I. & Georgescu, S. R. A New Horizon for Atopic
115 Dermatitis Treatments: JAK Inhibitors. *J Pers Med* **13** (2023).
116 https://doi.org:10.3390/jpm13030384

117 68 Ytterberg, S. R. *et al.* Cardiovascular and Cancer Risk with Tofacitinib in Rheumatoid Arthritis.
118 *The New England journal of medicine* **386**, 316-326 (2022).
119 https://doi.org:10.1056/NEJMoa2109927
120 69 Santoro, J. D. *et al.* Assessment and Diagnosis of Down Syndrome Regression Disorder:
121 International Expert Consensus. *Front Neurol* **13**, 940175 (2022).
122 https://doi.org:10.3389/fneur.2022.940175
123 70 Harris, P. A. *et al.* Research electronic data capture (REDCap)--a metadata-driven methodology
124 and workflow process for providing translational research informatics support. *J Biomed Inform*
125 **42**, 377-381 (2009). https://doi.org:10.1016/j.jbi.2008.08.010
126 71 Gu, Y. *et al.* High-throughput multiplexed autoantibody detection to screen type 1 diabetes and
127 multiple autoimmune diseases simultaneously. *EBioMedicine* **47**, 365-372 (2019).
128 https://doi.org:10.1016/j.ebiom.2019.08.036
129 72 Finck, R. *et al.* Normalization of mass cytometry data with bead standards. *Cytometry A* **83**, 483-
130 494 (2013). https://doi.org:10.1002/cyto.a.22271
131 73 Zunder, E. R. *et al.* Palladium-based mass tag cell barcoding with a doublet-filtering scheme and
132 single-cell deconvolution algorithm. *Nature protocols* **10**, 316-333 (2015).
133 https://doi.org:10.1038/nprot.2015.020
134 74 Hahne, F. *et al.* flowCore: a Bioconductor package for high throughput flow cytometry. *BMC*
135 *bioinformatics* **10**, 106 (2009). https://doi.org:10.1186/1471-2105-10-106
136 75 Chevrier, S. *et al.* Compensation of Signal Spillover in Suspension and Imaging Mass
137 Cytometry. *Cell Syst* **6**, 612-620 e615 (2018). https://doi.org:10.1016/j.cels.2018.02.010
138 76 Azad, A., Rajwa, B. & Pothen, A. flowVS: channel-specific variance stabilization in flow
139 cytometry. *BMC Bioinformatics* **17**, 291 (2016). https://doi.org:10.1186/s12859-016-1083-9

140 77 Love, M. I., Huber, W. & Anders, S. Moderated estimation of fold change and dispersion for
141 RNA-seq data with DESeq2. *Genome biology* **15**, 550 (2014). https://doi.org:10.1186/s13059-
142 014-0550-8
143 78 Subramanian, A. *et al.* Gene set enrichment analysis: a knowledge-based approach for
144 interpreting genome-wide expression profiles. *Proc Natl Acad Sci U S A* **102**, 15545-15550
145 (2005). https://doi.org:10.1073/pnas.0506580102
146 79 de Jesus, A. A. *et al.* Distinct interferon signatures and cytokine patterns define additional
147 systemic autoinflammatory diseases. *The Journal of clinical investigation* **130**, 1669-1682
148 (2020). https://doi.org:10.1172/JCI129301
149 80 Banchereau, R. *et al.* Personalized Immunomonitoring Uncovers Molecular Networks that
150 Stratify Lupus Patients. *Cell* **165**, 1548-1550 (2016). https://doi.org:10.1016/j.cell.2016.05.057
151
152

153 **Article and author information.**

154 **Acknowledgements:** This work was supported primarily by NIH grant R61AR077495. Additional
155 funding was provided by NIH grants R01AI150305 (J.M.E.), T32CA190216 (K.A.W.), 2T32AR007411-
156 31 (K.A.W.), UM1TR004399 (data generation and REDCap support), P30CA046934 (support of shared
157 resources), the Linda Crnic Institute for Down Syndrome, the Global Down Syndrome Foundation, the
158 Anna and John J. Sie Foundation, the Human Immunology and Immunotherapy Initiative, the University
159 of Colorado School of Medicine, the Boettcher Foundation, and Fast Grants. We are grateful to all research
160 participants and their families involved in the Human Trisome Project and the clinical trial. We thank
161 Lyndy Bush for administrative support, Dr. Kim Jordan and her team at the Human Immune Monitoring
162 Shared Resource for outstanding service in generation of the immune marker dataset, and Dr. Eric
163 Clambey and his team at the Flow Cytometry Shared Resource for outstanding service in generation of
164 the mass cytometry dataset. We are also grateful to the Colorado Translational and Sciences Institute and
165 the Colorado Multiple Institutional Review Board for assistance in all clinical research projects involving
166 the Crnic Institute. Special thanks to Michelle Sie Whitten, the team at the Global Down Syndrome
167 Foundation, Dr. John Reilly, and Dr. Ron Sokol for logistical support at multiple stages of the project.

168

169 **Author Contributions Statement:** A.L.R.: conceptualization, methodology, formal analysis, project
170 administration, data curation, visualization, investigation, resources, writing of manuscript; E.W.:
171 methodology, data curation, investigation, writing of manuscript; E.G.: methodology, data curation,
172 investigation, writing of manuscript; BEE: methodology, project administration, data curation,
173 investigation, writing of manuscript; K.R.W.: methodology, data curation, investigation, writing of
174 manuscript; K.P.S.: methodology, project administration, formal analysis, data curation, visualization,
175 investigation, writing of manuscript; P.A.: conceptualization, methodology, formal analysis, data curation,
176 visualization, investigation, writing of manuscript; K.A.W.: conceptualization, methodology,

investigation, writing of manuscript; R.E.G.: methodology, investigation, writing of manuscript; E.B.: methodology, investigation, writing of manuscript; H.R.L.: methodology, investigation, writing of manuscript; M.G.D.: methodology, investigation, formal analysis, data curation, visualization, writing of manuscript; N.P.E.: methodology, investigation, formal analysis, data curation, visualization, writing of manuscript; A.A.H.: conceptualization, methodology, project administration, investigation, writing of manuscript; B.M.: methodology, data curation, investigation, writing of manuscript; K.D.S.: methodology, investigation, visualization, writing of manuscript; L.P.: methodology, investigation, formal analysis, data curation, project administration, writing of manuscript; D.F.: methodology, investigation, formal analysis, data curation, project administration, writing of manuscript; M.D.G.: methodology, investigation, formal analysis, data curation, visualization, project administration, writing of manuscript; C.A.D.: conceptualization, methodology, data curation, investigation, project administration, writing of manuscript; D.A.N.: conceptualization, methodology, data curation, investigation, resources, project administration, writing of manuscript; J.M.E.: conceptualization, methodology, project administration, visualization, investigation, resources, writing of manuscript.

Competing Interests Statement: J.M.E. has provided consulting services for Eli Lilly Co., Gilead Sciences Inc., and Biohaven Pharmaceuticals and serves on the advisory board of Perha Pharmaceuticals. The remaining authors declare no competing interests.

196 **Supplementary File Legends.**

197 **Supplementary file 1.** (A) Cohort characteristics and (B) autoimmune conditions for Human Trisome
198 Project participants analyzed in this study.

199 **Supplementary file 2.** Autoantibody measurements of Human Tisome Project participants: (A) anti-
200 thyroid peroxidase (TPO) reactivity; (B) anti-nuclear antigen (ANA) reactivity; (C) SciLifeLabs
201 autoantigen peptide array data.

202 **Supplementary file 3.** (A) Minimum qualifying scores for skin conditions. (B) Cohort characteristics for
203 clinical trial participants.

204 **Supplementary file 4.** Adverse events for clinical trial participants.

205 **Supplementary file 5.** Skin pathology metrics for clinical trial participants: (A) Investigator's Global
206 Assessment (IGA); (B) Dermatology Life Quality Index (DLQI); (C) Severity of Alopecia Tool (SALT);
207 (D) Psoriasis Area and Severity Index (PASI); and (E) Eczema Area and Severity Index (EASI).

208 **Supplementary file 6.** (A) DS IFN scores; (B) Cytokine scores; (C) anti-thyroid peroxidase (TPO) titers;
209 (D) anti-transglutaminase (TG) titers; and (E) anti-thyroid stimulating hormone receptor (TSHR) titers for
210 clinical trial participants.

211 **Supplementary file 7.** Marker information for mass cytometry analysis.

212 **Supplementary file 8.** Clinical trial protocol.

213

214